



Developing a sequential cropping capability in the JULESv5.2 land–surface model

Camilla Mathison^{1,2}, Andrew J Challinor², Chetan Deva², Pete Falloon¹, Sébastien Garrigues^{3,4}, Sophie Moulin^{3,4}, Karina Williams¹, and Andy Wiltshire¹

¹Met Office Hadley Centre, FitzRoy Road, Exeter, EX1 3PB, UK

²School of Earth and Environment, Institute for Climate and Atmospheric Science, University of Leeds, Leeds, LS2 9AT, UK

³EMMAH (UMR1114), INRA, Avignon, France

⁴Université d'Avignon et des Pays de Vaucluse, UMR1114 – EMMAH, 84000 Avignon, France

Correspondence: Camilla Mathison (camilla.mathison@metoffice.gov.uk)

Abstract.

Sequential cropping (also known as multiple or double cropping) is a common feature, particularly for tropical regions, where the crop seasons are largely dictated by the main wet season such as the Asian summer monsoon (ASM). The ASM provides the water resources for crops grown for the whole year, thereby influencing crop production outside the ASM period.

5 Land surface models (LSMs) typically simulate a single crop per year, however, in order to understand how sequential cropping influences demand for resources, we need to simulate all of the crops grown within a year in a seamless way. In this paper we implement sequential cropping in a branch of the Joint UK Land Environment Simulator (JULES) and demonstrate its use at Avignon, a site that uses the sequential cropping system and provides over 15-years of continuous flux observations which we use to evaluate JULES with sequential cropping. In order to implement the method in future regional simulations where there may be large variations in growing conditions, we apply the same method to four locations in the North Indian states of Uttar Pradesh and Bihar to simulate the rice–wheat rotation and compare model yields to observations at these locations. JULES is able to simulate sequential cropping at Avignon and the four India locations, representing both crops within one growing season in each of the crop rotations presented. At Avignon the maxima of LAI, above ground biomass and canopy height occur at approximately the correct time for both crops. The magnitudes of biomass, especially for winter wheat, are underestimated and the leaf area index is overestimated. The JULES fluxes are a good fit to observations (r-values greater than 0.7), either using grasses to represent crops or the crop model, implying that both approaches represent the surface coverage correctly. For the India simulations, JULES successfully reproduces observed yields for the eastern locations, however yields are underestimated for the western locations. This development is a step forward in the ability of JULES to simulate crops in tropical regions, where this cropping system is already prevalent, while also providing the opportunity to assess the potential for other regions to implement it as an adaptation to climate change.



1 Introduction

Climate change is likely to impact all aspects of crop production affecting plant growth, development and crop yield (Hatfield and Prueger, 2015) as well as cropping area and cropping intensity (Iizumi and Ramankutty, 2015). The impact of climate change on agriculture has been the focus of several large collaborative projects such as the Agricultural Model Intercomparison and Improvement Project (AgMIP; Rivington and Koo (2010); Rosenzweig et al. (2013, 2014)) and the Inter-Sectoral Impact Model Intercomparison Project (ISIMIP; Warszawski et al. (2013, 2014)). These projects have highlighted the likelihood of competition between crops grown for food and those grown for bio-energy in order to mitigate climate change (Frieler et al., 2015). Petrie et al. (2017) discuss how the use of sequential cropping systems may have made it possible for populations in some areas to adapt to large changes in monsoon rainfall between 2200–2100 BC. These ancient Agricultural practices are common today across most tropical countries but may also be a useful adaptation, especially where traditionally mono-crop systems are currently used, in order to meet a future rising demand for food (Hudson, 2009) or the demand for bio-fuels. This sort of adaptation is already happening in some locations, Mueller et al. (2015) show that longer growing seasons in the extratropics have made the cultivation of multiple crops in a year at northern latitudes more viable, while warmer spring temperatures in the Brahmaputra catchment have allowed earlier planting of a winter crop leaving time for a second crop (Zhang et al., 2013).

Intercropping or sequential cropping allows farmers to make the most efficient use of limited resources and space in order to maximize yield potential and lower the risk of complete crop failure. These techniques also influence ground cover, soil erosion and chemical properties, albedo and pest infestation (Waha et al., 2013). Intercropping is the simultaneous cultivation of multiple crop species in a single field (Cong et al., 2015) while sequential cropping (also called multiple or double cropping) involves growing two or more crops on the same field in a given year (Liu et al., 2013; Waha et al., 2013). We use the term sequential cropping from here on to avoid confusion with other cropping systems. Sequential cropping systems are common in Brazil where the soybean–maize or soybean–cotton rotations are used (Pires et al., 2016) and for South Asia where the rice–wheat systems are the most extensive, dominating in many Indian states (Mahajan and Gupta, 2009), across the Indo-Gangetic Plain (IGP) (Erenstein and Laxmi, 2008) and Pakistan (Erenstein et al., 2008). States such as Punjab, Haryana, Bihar, Uttar Pradesh and Madhya Pradesh (Mahajan and Gupta, 2009) account for approximately 75 % of national food grain production for India. Rice–rice rotations are the second most prevalent crop rotation to rice–wheat rotations, these are typically found in the north eastern regions of India and Bangladesh (Sharma and Sharma, 2015) with some regions cultivating as many as three rice crops per year. The South Asia economy is highly dependent on the agricultural industry and other industries also with a high demand for water (Mathison et al., 2015). The most important source of water for this part of the world is the Asian Summer Monsoon (ASM), which typically occurs between June and September (Goswami and Xavier, 2005); this phenomena provides most of the water resource for any given year. The South Asia crop calendar is defined by the ASM which therefore has an important influence on the productivity across the whole year (Mathison et al., 2018) and therefore on crop production outside the Monsoon period.



The modelling of crop rotations is a common feature in soil carbon simulations (Bhattacharyya et al., 2007). Bhattacharyya et al. (2007) found that the rice–wheat rotation, common across the IGP, has helped maintain carbon stocks. However in recent years the yields of rice and wheat have plateaued leading farmers to diversify and include other additional crops in the rotation, potentially depleting carbon stocks. The modelling of crop rotations has also been common in the field of agricultural economics with work regarding sequential cropping being mainly to understand influences on decision-making; therefore focusing on short timescales and at the farm management level (Dury et al., 2012; Caldwell and Hansen, 1993).

Many dynamic global vegetation models (DGVMs), commonly used to study the effects of climate change, simulate a single crop per year, both for individual sites and gridded simulations. This may be due in part to some global observation datasets such as (Sacks et al., 2010) reporting only one growing period per year for most crops (Waha et al., 2012). MIRCA2000 (Portmann et al., 2010) include different cropping calendars for different regions, however rice and wheat are divided equally between the kharif and rabi seasons, when in reality wheat is only grown during the rabi season (Biemans et al., 2016). Waha et al. (2013) extend the Lund–Potsdam–Jena managed Land model (LPJmL-Bondeau et al. (2007)) to consider sequential cropping in Africa for two different crops. LPJmL is able to simulate sequential cropping in monoculture systems such as the rice–rice system grown in Bangladesh (Sharma and Sharma, 2015). In order to implement sequential cropping in LPJmL, Waha et al. (2013) specify different growing season periods for each crop in the rotation, where the growing period is given by the sum of the daily temperatures above a crop specific temperature threshold. They also specify the onset of the main rainy season as the start of the growing season using the Waha et al. (2012) method. Waha et al. (2013) find that when considering the impact of climate change, the type of cropping system is important because yields differ between crops and cropping systems. Biemans et al. (2016) also use a version of LPJmL, refined for South Asia, to estimate water demand and crop production for South Asia. Biemans et al. (2016) simulate sequential cropping by combining the output from two simulations with different kharif and rabi land-use maps and zonal sowing and harvest dates based on observed monsoon patterns. Biemans et al. (2016) find that accounting for the use of sequential cropping in this South Asia version of LPJmL improved the simulations of the demand for water from irrigation, particularly the timing of the demand. There are few land-surface models that are able to simulate sequential cropping but both Waha et al. (2013) and Biemans et al. (2016) have highlighted its importance in their simulations. It would be beneficial for more land-surface models to develop the capability to simulate different cropping systems and link crop production with irrigation both to improve the representation of the land surface in coupled models and to improve climate impacts assessments.

The JULES model is the land-surface scheme used by the UK Met Office for both weather and climate applications. It is also a community model and can be used in standalone mode; which is how it is used in the work presented here. JULES-crop, as described in Osborne et al. (2015) is a dual-purpose crop model intended for use both within standalone JULES, enabling a focus on food production and water availability applications as well as being the land-surface scheme within climate and earth system models. JULES in these larger models allows feed-backs from regions with extensive croplands and irrigation systems, like South Asia, to have an effect on the atmosphere e.g. via Methane emissions from rice paddies or evaporation from irrigated fields (Betts, 2005).



In this paper we describe and demonstrate the development and implementation of sequential cropping in JULES. This is part of a larger project to develop simulations for South Asia to understand the integrated impacts of climate change (Mathison et al., 2015, 2018) using state of the art RCM projections (Kumar et al., 2013; Mathison et al., 2013). This will improve understanding of the impacts of climate change and how they affect each other. There are many reasons for doing this including:

- 5 – improvement of simulations of those regions that use this cropping system currently,
- to understand the impact future climate change may have on this cropping system, for example in terms of water resources,
- and to consider the impact of adopting this cropping system for regions where it is not currently used but could be in the future.

10 The purpose of this study is to use the site in Avignon (France) described in Garrigues et al. (2015, 2018) to illustrate and evaluate the sequential cropping method implemented in JULES. The method is summarized by Fig. 1 and described in Sect. 3. We aim to show that the method is able to produce two crops in a single growing period and therefore provide a better representation of the real land surface at Avignon than previously possible using the crop model, rather than perform a detailed tuning exercise. Avignon is chosen because it has been observed and documented over several years (2001 to 2014), growing
15 a range of crops throughout this period. The continuous measurements of surface fluxes provided by this dataset are a unique resource for evaluating land surface models (LSMs) and for testing and implementing crop rotations in LSMs. Garrigues et al. (2015) use this dataset to evaluate LSM simulations of evapotranspiration using the interactions between soil, biosphere, and atmosphere scheme (ISBA) LSM (Noilhan and Planton, 1989) specifically, the version from Calvet et al. (1998); ISBA-A-gs.

 In this paper we focus on a two-crop-rotation between 2005 and 2012. In order to implement the method in a tropical region
20 where there is large variation in growing conditions, we apply the same method to four locations in the North Indian states of Uttar Pradesh and Bihar to simulate the rice-wheat rotation. These states are key producers of these crops using the sequential cropping system. The paper is structured as follows, Sect. 2 describes the JULES model and the method for implementing the sequential cropping system in JULES is outlined in Sect. 3. The simulations are described in Sect. 4, the results in Sect. 6 and Sect. 7 provides the discussion and conclusions.

25 2 Model description

JULES is a process-based model that simulates the fluxes of carbon, water, energy and momentum between the land-surface and the atmosphere. The model and the equations it is based on are described in detail in Best et al. (2011) and Clark et al. (2011). JULES treats each vegetation type as a separate tile within a gridbox with each one represented individually with its own set of parameters, independent fluxes and interactions with the atmosphere. Prognostics such as leaf area index (LAI)
30 and canopy height are therefore available for each tile. However the air temperature, humidity and windspeed are treated as homogenous across a gridbox and precipitation is applied uniformly over the different surface types of each gridbox. Below the



surface the soil type is also uniform across each gridbox. The parametrisation of crops in JULES (JULES-crop) is described in detail in Osborne et al. (2015) and Williams et al. (2017); the main aim of JULES-crop is to improve the simulation of land-atmosphere interactions where crops are a major feature of the land-surface (Osborne et al., 2015).

The development of the crop is controlled by the cardinal temperatures, these define the temperature range within which each crop is able to develop; these are the base temperature (T_b), maximum temperature (T_m) and optimum temperature (T_o) and specific for each crop. The cardinal temperatures and the 1.5m tile temperature (T) are used to calculate the thermal time i.e. the accumulated effective temperature (T_{eff}) to which a crop is exposed, as defined in Equation 1 (Osborne et al., 2015). Table 3 summarises the settings for these temperatures used in this analysis.

$$T_{eff} = \begin{cases} 0 & \text{for } T < T_b \\ T - T_b & \text{for } T_b \leq T \leq T_o \\ (T_o - T_b)(1 - \frac{T - T_o}{T_m - T_o}) & \text{for } T_o < T < T_m \\ 0 & \text{for } T \geq T_m \end{cases} \quad (1)$$

Crop development can also be affected by the length of the day, this is called photoperiod sensitivity and is controlled by two parameters in the model; the critical photoperiod (P_{crit}) and the sensitivity of a specific crop development rate to photoperiod (P_{sens}). The critical photoperiod defines the threshold optimum photoperiod for crop development, this typically only affects the crop during the vegetative phase, ie. before flowering (Penning de Vries et al., 1989). For some crops progress toward flowering is slowed if the day length is less than or greater than this specific photoperiod (Osborne et al., 2015). These parameters are used to define the overall effect of the photoperiod on the crop called the relative photoperiod effect, RPE described by Equation 2. In these simulations, as in (Osborne et al., 2015), the effect of photoperiod is not included i.e. P_{sens} is set to 0 and therefore RPE is equal to 1.0.

$$RPE = 1 - (P - P_{crit})P_{sens} \quad (2)$$

The RPE is then used to calculate the rate of crop development described by Equation 3.

$$\frac{dDVI}{dt} = \begin{cases} \frac{T_{eff}}{TT_{emr}} & \text{for } -1 \leq DVI < 0 \\ (\frac{T_{eff}}{TT_{veg}})RPE & \text{for } 0 \leq DVI < 1 \\ \frac{T_{eff}}{TT_{rep}} & \text{for } 1 \leq DVI < 2 \end{cases} \quad (3)$$

where TT_{emr} is the thermal time between sowing and emergence, TT_{veg} and TT_{rep} are the thermal time between emergence and flowering and between flowering and maturity respectively. These are calculated using a temperature climatology from the driving data and sowing dates from observations or a reliable dataset to ensure that the crop reaches maturity on average by the harvest date, the values used in these simulations are given in Tables 4 and 5. In order to simulate the characteristics of a



typical sequential cropping location using JULES we have implemented modifications to both JULES-crop and the irrigation code, these are described here. In order to simulate crops in sequence on the same gridbox, the first crop must no longer be in the ground so that the second one can be sown. The use of a latest harvest date, forces the harvest of the first crop regardless of whether it has reached maturity or not to make certain of this. These modifications are controlled using the `l_croprostate` switch (see table 1). Therefore `l_croprostate` ensures the following:

- All crops are initialized at the start of a simulation so that they can be used later when they are needed within the crop rotation being modelled.
- If JULES is simulating a crop rotation, the user must supply a latest harvest date so that the first crop is harvested before the second crop is sown (a latest harvest date can also be specified without using `l_croprostate`).

The current JULES default for irrigation allows individual tiles to be specified (when `frac_irrig_all_tiles` is set to false) but the irrigation is applied as an average across a gridbox and therefore actually occurs across tiles. The flag `set_irrfac_on_irrtiles` restricts the irrigation to the tiles specified by `irrigtiles` only (see table 1). This new functionality is needed because many locations that include crop rotations include crops that both do and do not require irrigation.

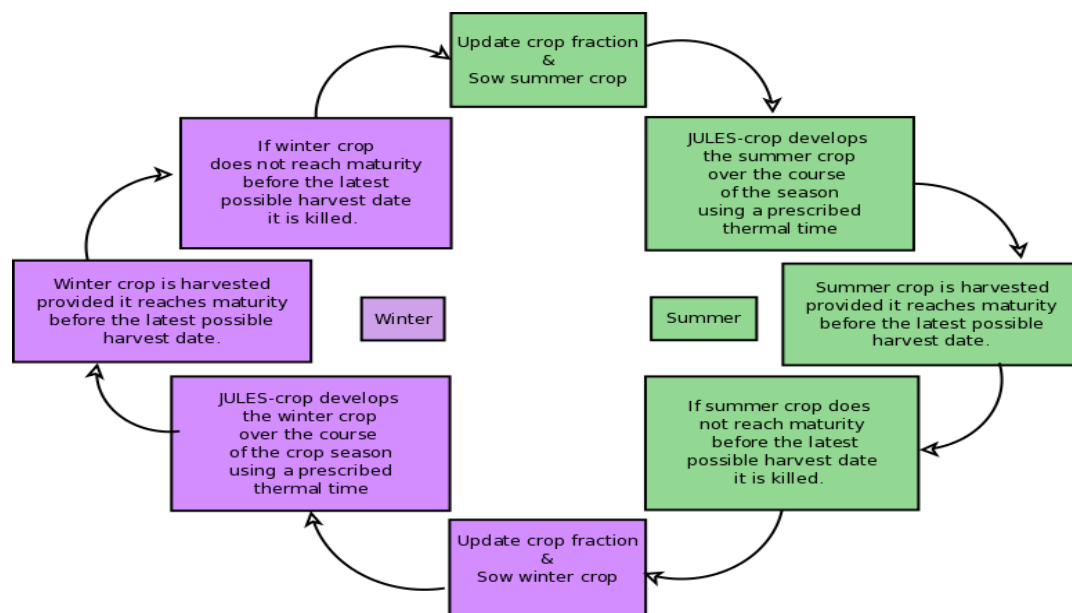


Figure 1. A flow chart showing the process followed to carry out the crop rotation in JULES.

3 Method for sequential cropping in JULES

The sequential cropping method implemented into JULES as part of this study is illustrated by the flow chart in Fig. 1 and described here using the Avignon site simulation. The Avignon site is a point run which is assumed to be entirely used to



grow sorghum (in summer) and winter wheat (in winter). JULES updates the fraction of the site that is allocated to sorghum (winter wheat) just before the sowing date so that the appropriate crop occupies the whole of the site. The fraction of the site that is sorghum (winter wheat) is prescribed in the Avignon case using observed sowing and harvest dates. Once the fraction is updated the crop is sown, it then develops between the stages of; sowing and emergence, emergence and flowering and

5 flowering and maturity. The crop model integrates an effective temperature over time as the crop develops through these stages with the carbon partitioned according to the DVI (see Sect. 2). The effective temperature (see Eq. 1) is a function of air or leaf temperature and differs between models. The DVI is a function of the thermal time since emergence, therefore $DVI = -1$ is sowing, 0 is emergence and 1 is flowering. Maturity and therefore harvest occurs at a DVI of 2 (Osborne et al., 2015). The integrated effective temperature in each development stage is referred to as the thermal time of that development stage (see

10 Sect. 2, Eq. 1 and Osborne et al. (2015); Mathison et al. (2018)). It is recommended for sequential cropping to prescribe a latest possible harvest date for those instances where the crop does not develop quickly enough and therefore does not reach maturity before the next crop in the rotation is due to be sown. The latest possible harvest date forces the removal of the first crop before the crop fraction is reassigned, ensuring that crops that are adjacent in time do not occupy the same area at the same time. This value can be assigned an observed harvest date if this is known or it can be the day before the next crop in

15 the rotation is due to be sown. The flow chart shown in Fig. 1 is equally applicable to the India simulations. Rice is therefore represented by the summer crop (green boxes) and wheat is represented by the winter crop (purple boxes). This method could be extended to include as many crops as occurs in a rotation at a particular location.

4 Model simulations

The simulations are divided into two sections. Section 4.1 applies the method to a well observed site in order to describe and

20 demonstrate how the sequential cropping method works and evaluate it against observations at this location. Section 4.2 applies the method to points in Northern India where this cropping system is commonly used. The parameter settings and switches used in JULES for the simulations in this study are provided in tables 1, 2 and 3. The Avignon and India simulations use the same settings wherever possible, these are provided in Table 1 (see Avignon settings and India settings columns). The PFT parameter settings are also broadly the same between simulations, with the majority of these from Osborne et al. (2015) and

25 therefore based on natural grasses. The crops are different between the two sets of simulations with winter wheat and sorghum at the Avignon site and spring wheat and rice at the India locations. The pft parameters used in this study that govern V_{cmax} ; including the lower (T_{low}) and upper (T_{upp}) temperatures for photosynthesis, n_{eff} and $n_l(0)$ are tuned to the maximum leaf assimilation expression from Penning de Vries et al. (1989) (see Table 2) for each crop. These values are consistent with the wider literature (Hu et al., 2014; Sinclair et al., 2000; Olsovska et al., 2016; Xue, 2015; Makino, 2003; Ogbaga, 2014).

30 The respiration parameters, μ_{rl} and μ_{sl} are from nitrogen concentrations given in Penning de Vries et al. (1989). The crop parameters are mainly from Osborne et al. (2015), with maize parameters used for sorghum (see Sect. 4.1) except for the cardinal temperatures which are from Nicklin (2012) (see Table 3).



The calculation of the soil moisture availability factor (see Table 2) is different between the Avignon and India simulations. In the Avignon simulations we assume that the total depth of the rootzone d_r is 1.5 m, equivalent to the observed average maximum root depth over all of the years at the Avignon site. The soil moisture availability factor is then calculated using this maximum root depth together with the average properties of the soil. The India point simulations assume an exponential root distribution with an e-folding depth d_r of 0.5 m because we do not have an observed root depth for these locations. The individual simulations are described in more detail in Sect. 4.1 and Sect. 4.2 for the Avignon and India simulations respectively.

4.1 Avignon site simulation

The Avignon "remote sensing and flux site" of the National Institute Agronomic Research (INRA) described in Garrigues et al. (2015, 2018), provides a well studied location with several years of crop rotation data. We focus on the period with a rotation of just two crops; winter wheat-sorghum between 2005 and 2012. The aim of simulating the crops at this site is to illustrate that the new sequential cropping functionality in JULES can simulate more than one crop within a year and reproduce the correct growing seasons for each crop. We evaluate JULES with sequential crops and grasses representing crops against the observed fluxes. We are not aiming to provide a perfect representation of the two crops at this site, this would require significant further work and model tuning. We have therefore not added specific parameterizations for the crops at Avignon but used existing crops within the model. Therefore Sorghum is largely based on the maize crop (as discussed earlier) as this is also a C4 crop and it is already available in JULES. We also use the existing spring wheat parameterization to represent the C3 winter wheat crop at Avignon.

The Avignon JULES simulation (referred to from here on using AviJUL) is driven using the meteorological site observations outlined in Sect. 5.1 and Garrigues et al. (2015, 2018) using a half hourly timestep. The irrigation is only applied to the summer Sorghum crop; this is included in the rainfall observations used to drive Avi-JULES. Therefore the irrigation and other settings governing irrigation are not switched on in JULES for the Avignon site simulations (See Table 1, column 'Avignon settings'). We include simulations for the Avignon site where the crops are represented by grasses (AviJUL-grass) for comparison with the simulations that use the new sequential cropping method implemented in the JULES-crop model (AviJUL-sqcrop). In the AviJUL-grass simulations the LAI and the canopy height are prescribed from observations in order to capture the growing seasons correctly without the crop model and the pft parameters are adjusted to be the same as the crops. In the AviJUL-sqcrop simulations the LAI and the canopy height are calculated by the model. Observed sowing and harvest dates from Garrigues et al. (2015) are used to calculate the thermal time requirements for each crop, these are provided in Table 4. During the periods between each crop, the ground is mostly bare (Garrigues et al., 2018).

4.2 India Simulations

The India simulations focus on the north Indian states of Uttar Pradesh and Bihar. These states are key producers of rice and wheat in India and the use of a rice-wheat rotation is prevalent in this part of India (Mahajan and Gupta, 2009). The sequential cropping system in this region involves growing rice during the wet monsoon months and an irrigated wheat crop during the dry winter. The wheat varieties grown in this region are spring wheat, this is an important distinction as spring wheat does



not require a vernalization period which is important for winter wheat varieties (Griffiths et al., 1985; Robertson et al., 1996; Mathison et al., 2018). We select four points across these two states in order to gain understanding of the model response, particularly in terms of yield, to the variation in the conditions across the two states. Point simulations allow more in depth analysis than a complete regional simulation, in order to inform future regional simulations using this sequential cropping
 5 method. The locations of the selected points are shown on a map of the surface altitude for South Asia in Fig. 2 (a). The driving data used for these four point simulations is from an RCM simulation run for South Asia for the period 1991–2007 as described below. Figure 2 (b, c and d) show a close-up view of the locations selected. Map (b) in 2 shows the average total monsoon precipitation for the 1991-2007 period while (c) and (d) show the average minimum and maximum temperatures respectively to illustrate that these four points are representative of the climate of the wider Uttar Pradesh - Bihar region.

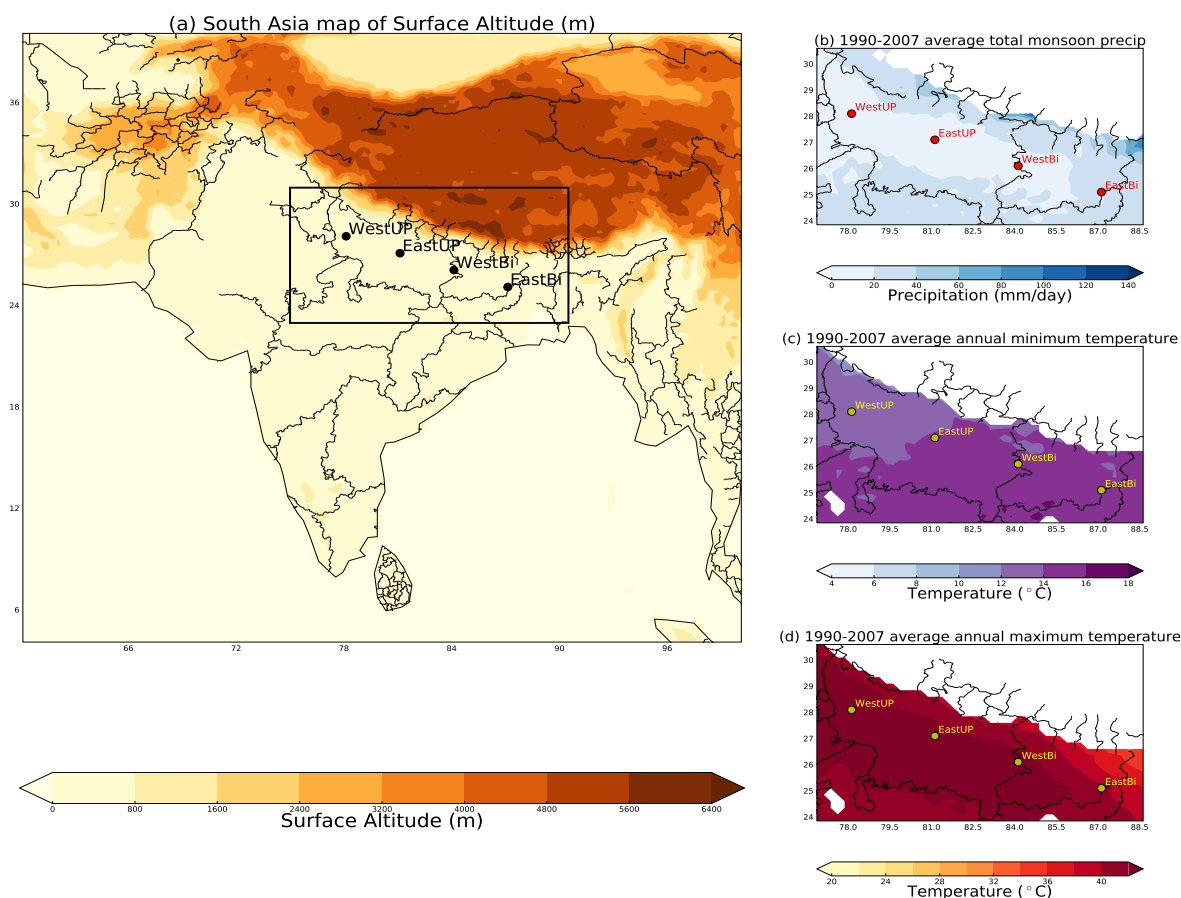


Figure 2. A map showing the location of the point simulations in the wider context of India on a map of the surface altitude (a) from the regional climate model that is used in the JULES simulations. The same points are shown in three smaller maps (b,c,d) that zoom in on the two states of Uttar Pradesh and Bihar. Map (b) shows the total monsoon precipitation, map (c) shows the minimum temperature, and map (d) the maximum temperature averaged for the period 1991-2007.



JULES is run using a 3-hourly timestep using driving data from ERA-interim (Dee et al., 2011; Simmons et al., 2007) downscaled to 25 km using the HadRM3 regional climate model (RCM-Jones et al. (2004)). This RCM simulation is one of an ensemble of simulations produced for the EU-HighNoon FP7 project for the whole of the Indian subcontinent (25 N, 79 E–32 N, 88 E) for the period 1991–2007. The HighNoon simulations are described in detail in previous publications such as Kumar et al. (2013) and Mathison et al. (2013, 2015). HadRM3 provides more regional detail to the global data with lateral atmospheric boundary conditions updated 3-hourly and interpolated to a 150 s timestep. These simulations include a detailed representation of the land surface in the form of version 2.2 of the Met Office Surface Exchange Scheme (MOSESv2.2; Essery et al. (2001)). JULES has been developed from the MOSESv2.2 land surface scheme and therefore the treatment of different surface types is consistent between the RCM and JULES (Essery et al., 2001; Mathison et al., 2015). Sowing dates are prescribed using climatologies calculated from the observed dataset, Bodh et al. (2015), from the government of India, Ministry of Agriculture and Farmers welfare. Thermal times are calculated using these climatological sowing and harvest dates from Bodh et al. (2015) and a thermal climatology from the model simulation as described in Osborne et al. (2015), the values used in the simulations here are provided in Table 5. In the JULES point simulations only wheat is irrigated, the settings used for this are provided in Table 1 (column ‘India settings’).

5 Observations

5.1 Avignon observations

The length and detail of the observation record at the Avignon site means it is an ideal site to demonstrate the method being implemented in JULES for simulating sequential cropping. High resolution meteorological data, important for the practicalities of running the JULES model is available on a half hourly basis; this includes air temperature, humidity, windspeed and atmospheric pressure at a height of 2m above the surface. Cumulative rainfall, radiation measurements and sensible (H) and latent heat (LE) fluxes are also available, with the latter flux measurements enabling the evaluation of the JULES fluxes. Cumulative evapotranspiration (ET) are derived from the half hourly LE measurements. The observations for evaluating the model include soil measurements of soil moisture along with plant measurements including canopy height (measured every 10 days), above ground dry weight biomass (taken at four field locations) and LAI; biomass and LAI are destructive measurements repeated up to six times per crop cycle (Garrigues et al., 2015). More information is documented in Garrigues et al. (2015) regarding the site and the observations available.

5.2 India observations

Crop yield observations from the International Crops Research Institute for the Semi-Arid Tropics (ICRISAT, 2015)) provides seasonal yields for each crop for comparison with the point simulations. We also show average crop yield observations from Ray et al. (2012a) for three, 5-year periods between 1993 and 2007 (1993–1997, 1997–2003, 2003–2007) via Ray et al. (2012b). These data are based on previous publications Monfreda et al. (2008) and Ramankutty et al. (2008) and include the



period of the point simulations which are from 1991–2007. We show both of these datasets to highlight that there is a range in the estimates of yield for this region.

6 Results

6.1 Avignon site simulation

Figure 3 shows the timeseries of total above ground biomass (a), LAI (b) and canopy height (c) for the AviJUL-grass and AviJUL-sqcrop simulations. Figure 3 shows that the crops are developing throughout the crop seasons with maxima of biomass, LAI and canopy height occurring at approximately the correct time for both crops. The total above ground biomass from JULES is calculated from the sum of the stem, leaf and harvest carbon pools for each crop and plotted as a time series (dashed lines). Biomass observations are provided as a single timeseries with the crop type confirmed from the timing of the observations, these are plotted alongside the model represented by purple asterisks (see plot (a), Fig. 3). It is noticeable that the 2009 observed growing season for sorghum is much shorter than for the other two sorghum crop seasons (shown by the red solid line in Fig. 3 a, b and c). The 2009 sorghum crop is planted much later in the year compared to the other two sorghum seasons (2007 and 2011) but harvested at a similar time. This is because the variety of sorghum planted in 2009 is different to the variety planted 2007 and 2011 seasons. The 2009 variety is a fodder crop with a much larger LAI and a shorter growing season. JULES fits the biomass observations for 2009 well (see Fig. 3 plot a). JULES also closely fits the leaf area (see Fig. 3 plot b) and canopy height observations (see Fig. 3 plot c) for the 2009 Sorghum season, with differences between the simulations and observations maximum values of approximately $1 \text{ m}^2 \text{ m}^{-2}$ and 0.1 m respectively. In the 2007 sorghum season JULES overestimates the maximum LAI and canopy height by approximately two times the observations (see Fig. 3 plots b and c) and underestimates the total biomass (see Fig. 3 plot a) by about 30 %. For the 2011 season the JULES sorghum biomass equals the magnitude of the observations, however the maximum LAI is overestimated by four times in the model (similar to 2007) and the maximum canopy height is approximately two times the observed maximum. The canopy height is very close to observations for wheat in all four seasons, however the wheat LAI is overestimated and the biomass is underestimated in all years. The two wheat seasons of 2006 and 2010 are closer to the LAI observations than 2008 and 2012, however the underestimation of the biomass is greater for these seasons. For 2008 and 2012 the wheat biomass is closer to the observations but the overestimation in the LAI is greater. The increase in biomass for both crops through the start of the season follows the observations quite closely but in most years, especially for wheat, JULES does not accumulate enough biomass later in the crop season to reach the observed maxima.

The level of soil moisture that a plant begins to experience water stress at is reduced by the introduction of the variable p_0 ; this is a scaling factor used in the soil moisture stress calculation (Williams et al., 2018). The setting of p_0 and how this affects GPP at the First ISLSCP Field Experiment (FIFE) site in Kansas is discussed in detail in Williams et al. (2018). In addition Williams et al. (2017) suggest modifying the p_0 parameter to be 0.65 for the Mead site in Nebraska. In the simulations shown here p_0 is set to 0.5 (see Table 2) modified from the default setting of 0, as recommended by Allen et al. (1998). The way that vegetation in JULES uses water and its response to drought conditions is currently under investigation within the wider



JULES community as described in Williams et al. (2018) and Harper et al. (in preparation). The canopy height does not really change with the modification of p_0 from 0 to 0.5 (not shown), however biomass and LAI are more sensitive to changes in this parameter, this is apparent from comparison of Fig. 3, plots (a) and (b) with those from simulations that use the default setting provided in the Appendix (see Fig. A5 plots (a) and (b)). Setting p_0 to 0.5 marginally improves the JULES biomass fit to observations but results in a large over estimation of the wheat LAI compared with a setting of 0 which gives an LAI that is closer to the observations (see Fig. A5 plot b). The years with a large (small) LAI are also represented more closely for $p_0 = 0$. Garrigues et al. (2015) highlight that 2006 and 2008 are two atypical years with 2006 being very dry (256 mm of rain) and 2008 being very wet (500 mm of rain), these differing conditions could explain the large differences in observed LAI and biomass between the two years (Garrigues et al., 2015). The peaks in productivity shown in the LAI in Fig. 3, (b) are consistent with the two years (2006 and 2007) of observations of GPP, shown by the black line in Fig. 4, plot (a). The wheat crop is clearly shown in the GPP for 2006, although it is underestimated in all simulations (see Fig. 4). The decline in GPP at the end of the wheat season is quite close to the observations with AviJUL-grass (red line) being slightly early and AviJUL-sqcrop (blue line) being slightly late. In the sorghum season of 2007 the magnitude and timing of the maximum GPP for the AviJUL-sqcrop simulation are a good fit to observations (see Fig. 4, plot a and Fig. A1 plot b), although the increase in GPP for both simulations begins too early the decline is very close to the observations. The decline is very close to observations for the AviJUL-grass simulations too although the maxima are slightly too low and a little later than observed (see Fig. 4, plot a). This is quantified in Fig. A1 each of the simulations show a strong linear correlation with r -values of above 0.7 (see Fig. A1 plots (a) and (b) and the values in the GPP row of Table 6).

On the basis that p_0 has a positive impact on some aspects of the Avignon simulations it is likely that water stress is a factor in the simulations shown here. However there may be other factors not considered here, for example, the long periods of bare soil between between the winter and summer crops (e.g. July of 2006 to April of 2007). This could have a more significant impact on the crops grown in the following year in the model than in reality.

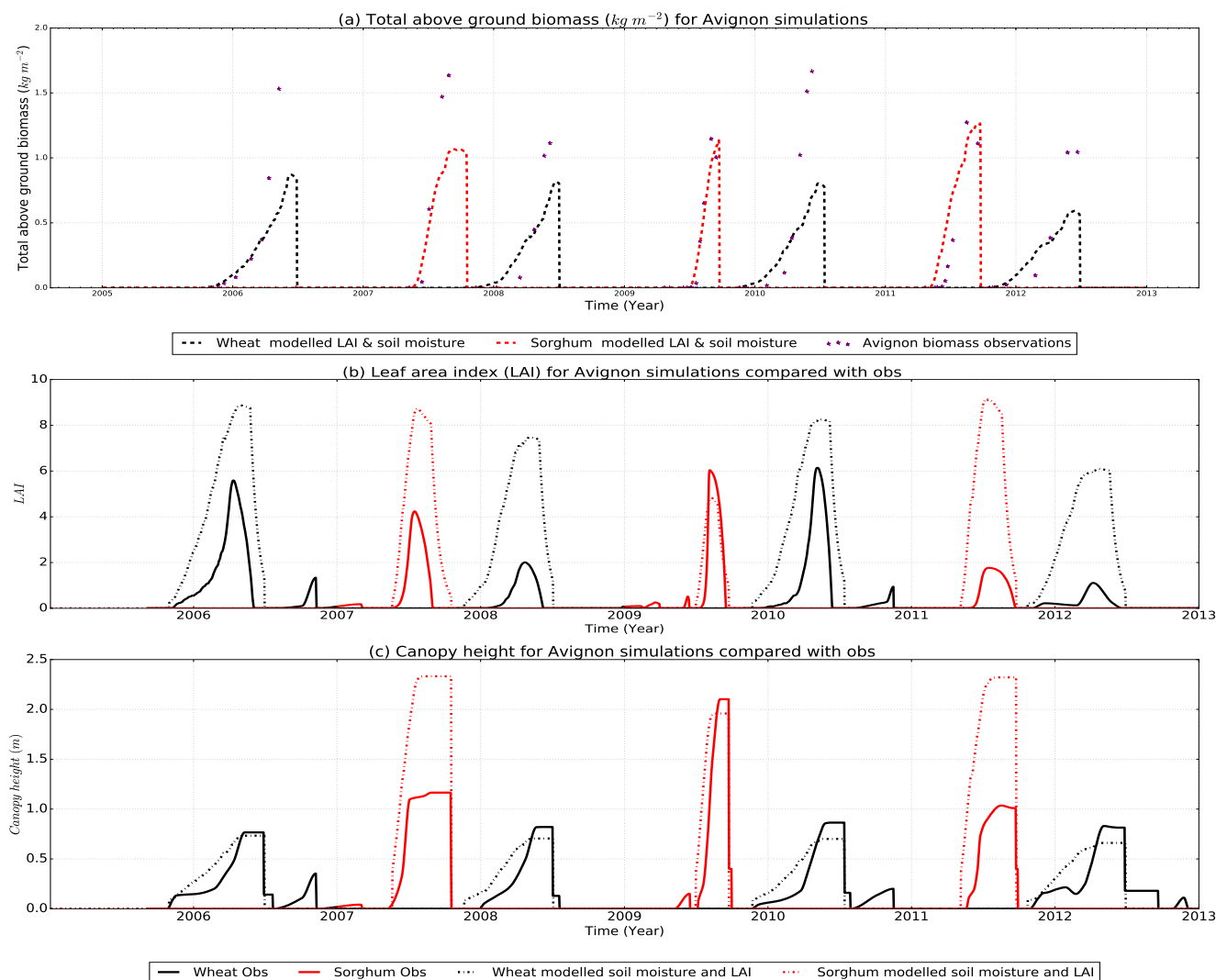


Figure 3. The timeseries of total above ground biomass (a), leaf area index (LAI) (b) and canopy height (c) for the Avignon site for wheat (black) and sorghum (red) for observations (solid lines) and simulations using the observed sowing and harvest dates: AviJUL-sqcrop and modelled soil moisture (dashed) for the period between 2005 and 2013 using observed sowing and harvest dates. Simulations with prescribed LAI and canopy height are not shown here as these follow the observed LAI and canopy height. Observed above ground biomass in plot (a) shown by purple asterisks

The H and LE fluxes are shown in Fig. 4, plots (b) and (c) respectively. The AviJUL-sqcrop (blue line) and the AviJUL-grass (red line) simulations follow each other closely which is reflected in the RMSE values and bias values for each simulation (see Table 6 and Figures A2 and A3 for H and LE comparisons respectively), these are generally comparable to those from Table 5 in Garrigues et al. (2015), which are LE : rmse of 52.4, bias of -11.8, and H : rmse of 56.2, bias of 17.6. The linear correlations shown for H and LE in Fig. A2 and Fig. A3 respectively, are strong for these simulations with r _values above



0.7, (see plots a and b). These values are comparable to those from Table 5 in Garrigues et al. (2015), which provides values of 0.8 for LE and 0.85 for H . The annual cycle of LE and H are shown in Fig. A4, a and b respectively. Figure A4 highlights how well the simulations capture the seasonal cycle, this is also evident in the timeseries shown in Fig. 4, plot b and c.

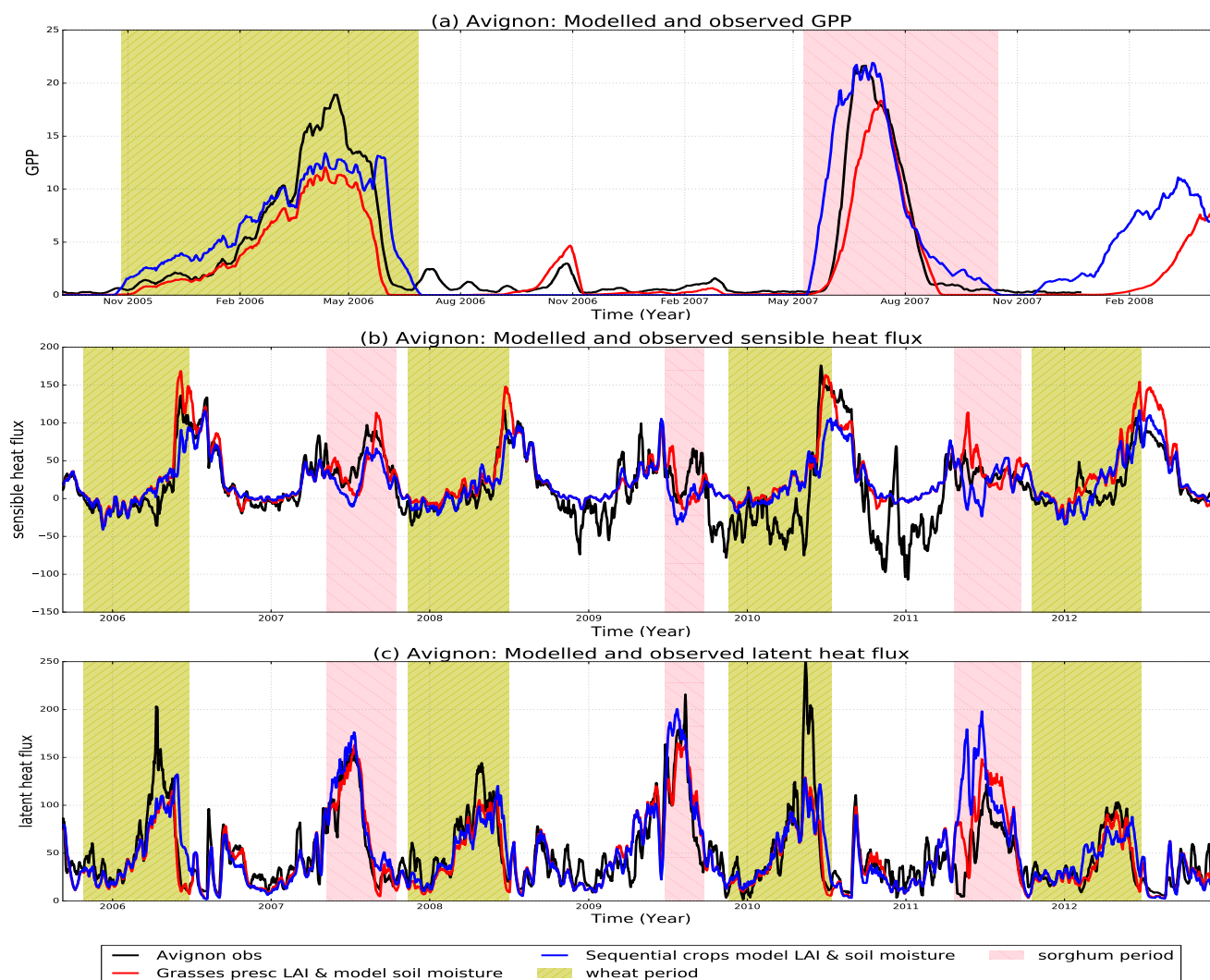


Figure 4. The timeseries of GPP (a), H (b) and LE (c) for the Avignon site compared with observations (black lines). H (b) and LE (c) heat fluxes show the whole period from 2005-2012, while GPP shows the period 2005-2008 due to availability of observations. The following model simulations are also shown: AviJUL-grass with prescribed LAI and modelled soil moisture (red), AviJUL-sqcrop with both soil moisture and LAI modelled (blue). In each plot a 10-day smoothing has been applied to the daily data.

Given that the soil moisture is important for these JULES simulations at Avignon, Fig. 5 plot (a) and (b) summarize the soil moisture conditions in these simulations. Figure 5, Plot (a) shows the available soil moisture in the top 1.0 m of the soil. The



observations are generally lower than the soil moisture in the simulations throughout most of the timeseries. The AviJUL-sqcrop simulation captures some of the larger dips in the available soil moisture but mostly follows the same patterns as AviJUL-grasses. The soil moisture availability factor shown in Fig. 5 plot b, shows that there are periods where the soil moisture stress is higher in the observations. Additional simulations that prescribe the soil moisture using these site observations (shown in Fig. 5) have an early decline in GPP (not shown), this is due to water stress acting as a scaling factor on net leaf assimilation. A closer look at the soil moisture timeseries on each of the four levels reveals that the top soil layer (not shown), with a depth of 10 cm, is much too variable in the model compared with the observations which are very stable. The AviJUL-sqcrop simulations follow the observations more closely in the other three soil layers capturing the timing of periods where the soil moisture is lower although not the magnitude. There is also a period in the second half of 2009 where the models simulate a drop in soil moisture in levels 1,2 and 3 that is not in the observations; this is evident in the available soil moisture in the top 1.0 m of the soil shown in Fig. 5, plot (a).

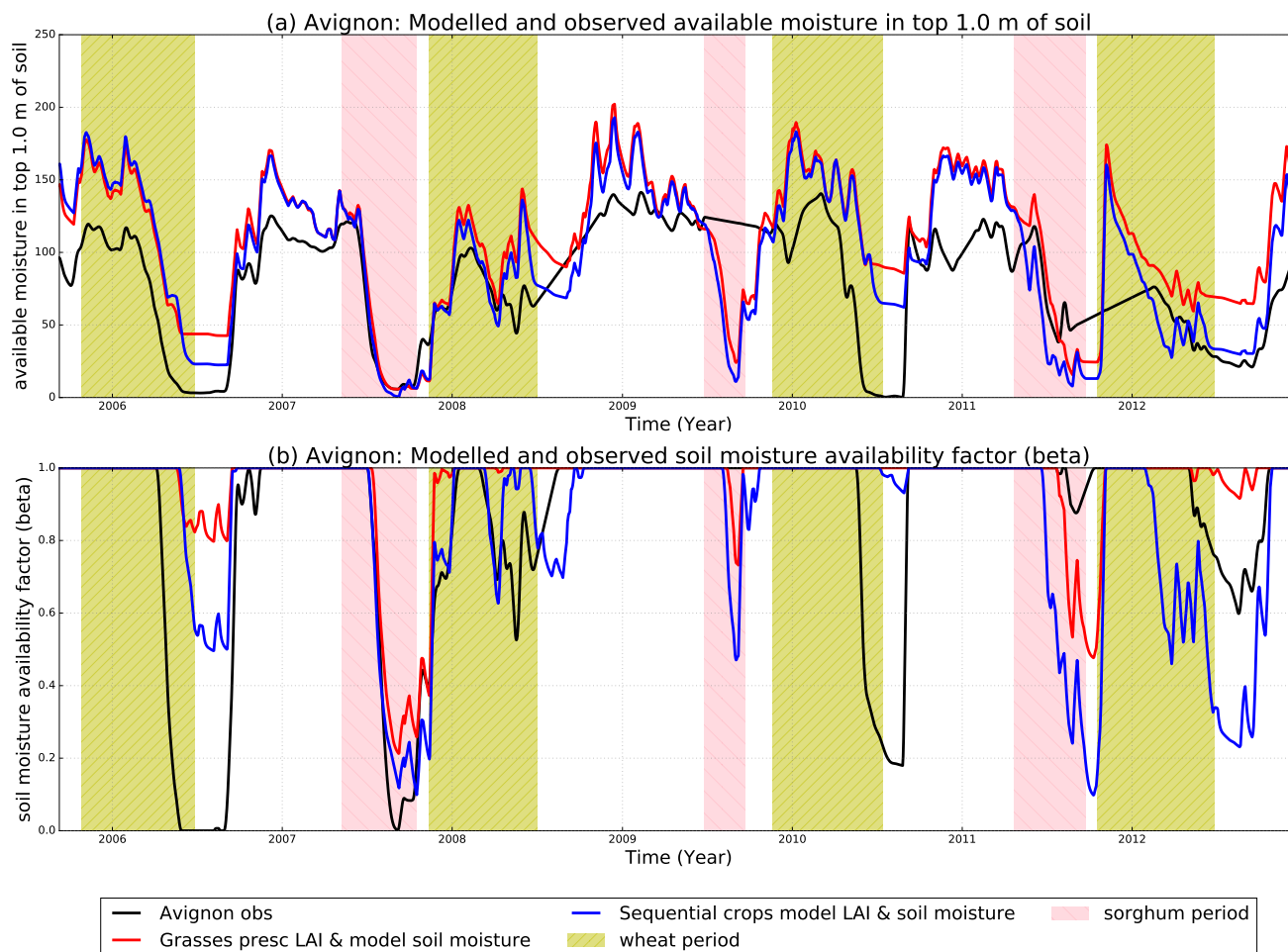


Figure 5. The timeseries of the available soil moisture in the top 1.0 m of soil and the soil moisture availability factor (Beta) for the Avignon site for 2005 to 2013 using observed sowing and harvest dates (black line). AviJUL-grass with modelled soil moisture shown in (red), AviJUL-sqcrop with modelled LAI and soil moisture (blue).

The Avignon simulation has shown that the method implemented for simulating sequential cropping in JULES provides two crops per year for several years. The representation of crops either using the crop model or using grasses to represent crops has a similar effect on the surface fluxes. The representation of soil moisture has a large effect in these simulations. As previously discussed the representation of soil moisture stress on vegetation in JULES is a known issue which is the subject of a large international collaborative effort (Williams et al., 2018; Harper et al., in preparation). The representation of individual crops at Avignon in JULES could probably be improved by having sorghum and winter wheat specific parameterizations in JULES, that are tuned to the crop varieties at this location. Such parameterizations are not available at the time of writing and would require significant further work to implement. It is clear that the 2009 variety of sorghum would also require different parameters to those for 2007 and 2011. However, the aim of presenting this simulation is to demonstrate the method rather than provide a



perfect representation of either of these crops. This site at Avignon is a valuable resource that will help develop and test future specific parameterizations for these crops and others that are also grown at this site. It is hoped that the suite that runs JULES at Avignon with and without sequential crops could become one of the 'golden' sites that is referred to in Williams et al. (2018) and thereby aid future development of JULES and other land surface and crop models to include a sequential cropping capability. In the following section we apply this same method to a range of locations that use the sequential cropping system in the north of India in order to implement this method for a regional tropical simulation.

6.2 India simulations

The four India points selected for analysis in this study are shown on a map of South Asia in Fig. 2 (plot a) with smaller inset plots (b, c and d) focusing on the sequential cropping region being considered across the states of Uttar Pradesh and Bihar.

- Figure 6 shows the differences in the timeseries of the average precipitation (a), temperatures (b), and vapour pressure deficit (VPD) (c) at each of these four points with the different crop seasons emphasized by the different colour shading (yellow for wheat and pink for rice) on each of the plots. The temperatures rarely reach the low temperatures of the t_{base} cardinal temperatures set in the model shown for rice (green) or wheat (orange) on Fig. 6 (b), however the high temperatures do exceed the maximum cardinal temperatures for these crops, especially those set for wheat. In general EastBi is cooler than the other points in more of the years with the two locations in Uttar Pradesh often being the warmest. The precipitation at each location is variable (see Fig. 6 plot a) and there appears to be a variation in the distribution of precipitation through the monsoon period which could be important for crop yields. Challinor et al. (2004), for example, found that in two seasons with similar rainfall totals, the distribution of the rainfall during the growing season strongly affected groundnut crop yield. There is also a clear seasonal cycle in the vapour pressure deficit (VPD), increasing toward the end of the wheat season and decreasing into the rice season. EastBi generally has the lowest VPD, with WestUP and EastUP usually the highest throughout the timeseries shown (see Fig. 6). These plots suggest that there is a gradual change in conditions from west to east across Uttar Pradesh and Bihar with increasing humidity and rainfall and decreasing maximum temperatures from west to east.

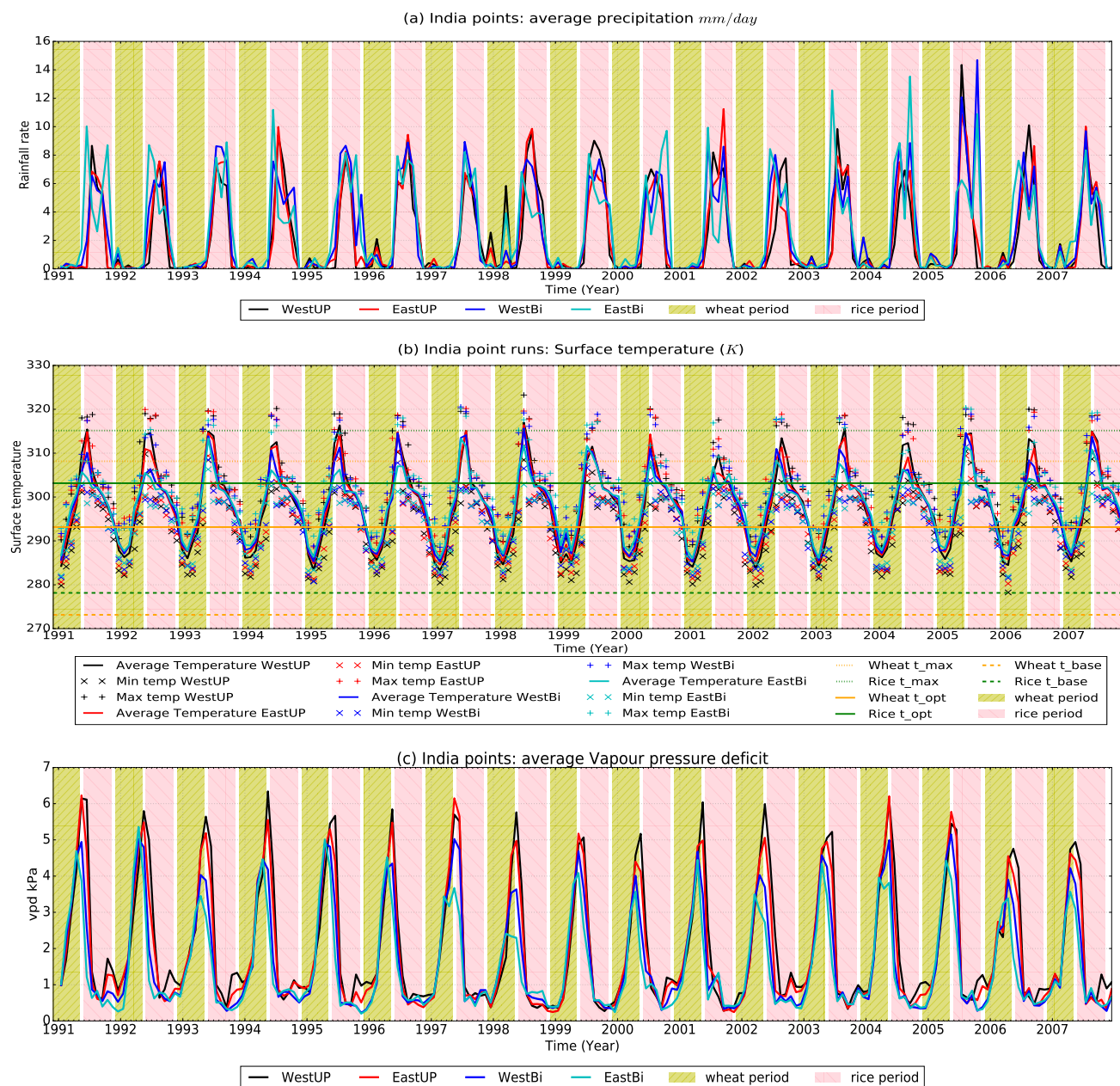


Figure 6. Timeseries of average precipitation (a), temperature (b), and vapour pressure deficit (c) at each of the India sites shown by the solid lines (WestUP-black, EastUP-red, WestBi-blue and EastBi-cyan). Plot (b) also shows the minimum ('x') and maximum ('+') temperatures for each of the locations for each month together with the JULES cardinal temperatures (horizontal lines) for rice (green) and wheat (orange): Max temperatures (dotted line), optimum temperatures (solid line) and base temperatures (dashed line).



The sequential cropping simulations at these India sites produce both a rice and wheat crop (see Fig. 7, with red representing rice and black representing wheat), and a crop DVI regularly showing that the crop reaches 2 (see Fig. B2), indicating maturity. This indicates that JULES is growing both wheat and rice at each of these locations within one growing season and is therefore simulating the sequential cropping rotation. We first consider if the main crop characteristics such as LAI and canopy height are realistic. This is important, especially where the results are to be applied to analysis of future water resource requirement, where an overestimation (underestimation) of size or leaf area for a crop could skew the results towards a higher (lower) resource requirement. In these simulations the canopy height (see Fig. B3) for both rice and wheat at each location is between 0.5 and 0.7 m (see Fig. B3) which is an expected value for a typical crop, as described in (Penning de Vries et al., 1989). Figure 8 shows the LAI for each of the four locations, indicating that the wheat LAI from JULES is between 5 and 7 m^2m^{-2} across the locations; this is also an expected value for a crop according to Penning de Vries et al. (1989). Rice LAI is lower (between 2 and 4 m^2m^{-2}) with the lowest values for WestUP, slightly increasing from west to east locations. For WestUP particularly, rice (red solid line) has a small LAI (see Fig. 8) but it generates a yield (red asterisks Fig. 7) that falls within the range of the observations for each year, however wheat (black solid line) generates an LAI that is closer to expected values but a smaller yield compared with observations (see Fig. 7, black asterisks). WestUP has the least available soil moisture, lowest rainfall and higher temperatures than the other locations, yet the observed yields and therefore the actual productivity are higher than the other locations.

Figure 10, plot (c) shows the NPP for each of the locations. The NPP shows a decline, particularly for wheat, which begins relatively early in the season, this is due to the overall plant respiration being relatively high (see Fig. B5), the leaves senescing and therefore not photosynthesizing and the remobilisation of carbon to the harvest pool (see Fig. 9). This early decline in NPP could have a direct impact on yield in the model.

Figure 7 shows the yields from JULES (asterisks) overlaid on the curve of the harvest pool (solid lines) for each crop together with two observation datasets. The datasets are from ICRISAT (2015) shown by the filled circles and Ray et al. (2012a) by filled triangles (see Fig. 7) highlight that there is a spread between yield estimates for this region. The model (asterisks on Fig. 7) tends to underestimate the wheat yield for most years at the WestUP location (average bias across both datasets of $-0.13 kg m^{-2}$). Rice is more mixed for WestUP, falling within the range of the observations in more than half of the years (average bias $-0.064 kg m^{-2}$). The average bias across both observation datasets is much smaller for the other locations with rice and wheat yields within the range of the observations for most years for both EastUP and WestBi (average bias across both crops at these locations ranges from -0.07 to $0.02 kg m^{-2}$). During the second half of the simulation the wheat yield is underestimated by the model more often at EastUP but this is just the occasional year for WestBi and does not occur at all for EastBi. For EastBi the rice yields are often toward the top of the range provided by the two observed datasets but still within the range of the observations (see Fig. 7), this gives on average a positive bias of 0.06 for rice and 0.02 for wheat. However the observed yields at EastBi are lower than the other locations, where the cooler wetter conditions should be more conducive to achieving higher yields but these are neither observed or modelled.

The wheat crop is irrigated in these simulations and therefore the soil moisture availability factor is equal to 1.0 during the wheat season (see Fig. 11). Therefore suggesting it is not water stress that influences the wheat yields in these JULES



simulations. The models underestimation of the high WestUP wheat yield (compared to EastBi) is therefore likely to be due to a combination of factors. One explanation is likely to be the differing management practices between the two states of Uttar Pradesh and Bihar. Uttar Pradesh is characterized by high agricultural productivity with effective irrigation systems (Kumar et al., 2005) and early adoption of new management practices (Erenstein and Laxmi, 2008). Bihar on the other hand has lower agricultural productivity, farms tend to be smaller and more fragmented, irrigation systems are less effective (Laik et al., 2014) and adoption of new technology is also slower due to the lack of available machinery (Erenstein and Laxmi, 2008). Yield gap parameters are included in many crop models in order to account for the impact of differing nutrient levels, pests, diseases and non-optimal management (Challinor et al., 2004); thus explaining the difference between potential and actual yield under the same environment Fischer (2015); this is not included in these simulations.

At the western locations, the humidity is lower (higher VPD) and the temperatures are higher; these conditions may provide another contributory factor for the model underestimating the yields there. The humidity in the simulations could be lower in these simulations than in reality for two reasons; firstly we are running JULES in standalone mode. This means the land-surface and therefore the crop is unable to influence the atmosphere through evaporation because the humidity is prescribed by the driving data at each timestep. Secondly the driving data is from an RCM that does not include irrigation (Mathison et al., 2015) so the humidity in the driving data is not modified by evaporation due to irrigation. We are therefore missing the part of the water cycle that allows evaporation from the surface to affect the humidity. This region is intensively irrigated (Biemans et al., 2013) which means that there is a significant contribution from the evaporation due to irrigation and the recycling of water into precipitation (Harding et al., 2013; Tuinenburg et al., 2014) that cannot be accounted for here. Tuinenburg et al. (2014) estimate that as much as 35 % of the evaporation moisture from the Ganges basin is recycling within the river basin. We hypothesize that the VPD may be too high in our forcing data and this could be affecting the model yields at this location (Ocheltree et al., 2014). An additional simulation completed as a sensitivity test to see if low humidity in the driving data could be affecting the model yields, did have the effect of increasing NPP and yield for WestUP suggesting this hypothesis is worthy of further investigation. However, how plants respond to high VPD is still the source of a great deal of debate (Medina et al., 2019). There are two theories for the plant response to high VPD; the first is stomatal conductance decreases as VPD increases because of an increase in transpiration that lowers the leaf water potential (Streck, 2003; Ocheltree et al., 2014; Medina et al., 2019) rather than a direct response to the humidity. In this first theory if the rate of movement of moisture out of the stomata cannot be met by the vascular structure of the plant then the plant will become water stressed (Streck, 2003). The second theory is that there is a direct stomatal response to high VPD where stomatal conductance decreases as VPD increases, with abscisic acid (ABA) in the leaves probably triggering the response (Streck, 2003). However, Streck (2003) suggest that a direct response to VPD is probably contingent on the plant being exposed previously to water stressed conditions. (Medina et al., 2019) investigate the response to high VPD of both irrigated and rainfed C3 and C4 grasses and find evidence of the direct response to VPD in some species; in fact there are published results that support both of these hypotheses. Further investigation is needed to confirm exactly why the simulation at WestUP does not achieve the observed yields.

The total above ground biomass for both crops shown in Fig. B1 are comparable with each other and with the values simulated for wheat at Avignon. Figure 9 shows the evolution of the carbon pools for wheat and rice at each of the India



locations for the years between 1998 and 2001 in order to examine the evolution of the carbon pools more closely by looking at a smaller number of crop seasons. The root carbon pool is a significant proportion of the total wheat biomass, larger than the rice root carbon pool, for rice it is the stem carbon pool that constitutes the larger proportion of the total biomass. As expected the leaf carbon drops away during senescence (this occurs when the DVI reaches 1.5 in these simulations) and the leaf carbon is remobilized to the harvest pool but the stem (for rice) and the roots (for wheat) remain high until harvest. Where the level of carbon remains high for a particular carbon pool, the respiration also remains high. It is therefore possible that the carbon partitioning after flowering requires some revision for JULES-crop simulations, especially for wheat. The carbon partitioning in the model may also be affecting the model wheat yields and may provide another avenue for investigation in addition to those discussed so far. The temperatures during the wheat season shown in Fig. 6 rise rapidly often reaching temperatures that are well above the maximum for the development of wheat by the expected harvest date. These high temperatures may speed up the rate at which wheat matures and therefore shorten the senescence period too much in the model bringing forward the harvest date without giving the yield carbon pool time to increase. The total plant respiration is also shown in Fig. B5 with the respiration for each crop and carbon pool shown in Fig. B4. Usually toward the end of the wheat season the plant respiration declines, as carbon is remobilized to the harvest pool which does not respire and the leaves senesce; this results in a decline in the respiring biomass. The rice plant respiration (see Fig. B5) has a dip in the middle of the 2001 season that only occurs in EastBi, this is caused by a drop in the leaf respiration shown in Fig. B4 plot (d). The drop in leaf respiration is related to changes in temperature, precipitation and VPD at this location. Usually the temperature timeseries shows an increase through the wheat season which peaks during the short period between the two crops and then declines into the rice season. In 2001 there is an initial decline but then a sharp rise in temperature before it then follows its usual decline into the winter wheat season. The rise in temperature is at the same time as the spike in VPD at EastBi (see Fig. 6 plot c). The usual fall in temperature is therefore much later in the 2001 rice season which is accompanied by a significant drop in precipitation in the middle of the monsoon for EastBi which does not occur at the other locations for this year.



India point runs: Carbon in harvested parts of crop ($kg\ m^{-2}$)

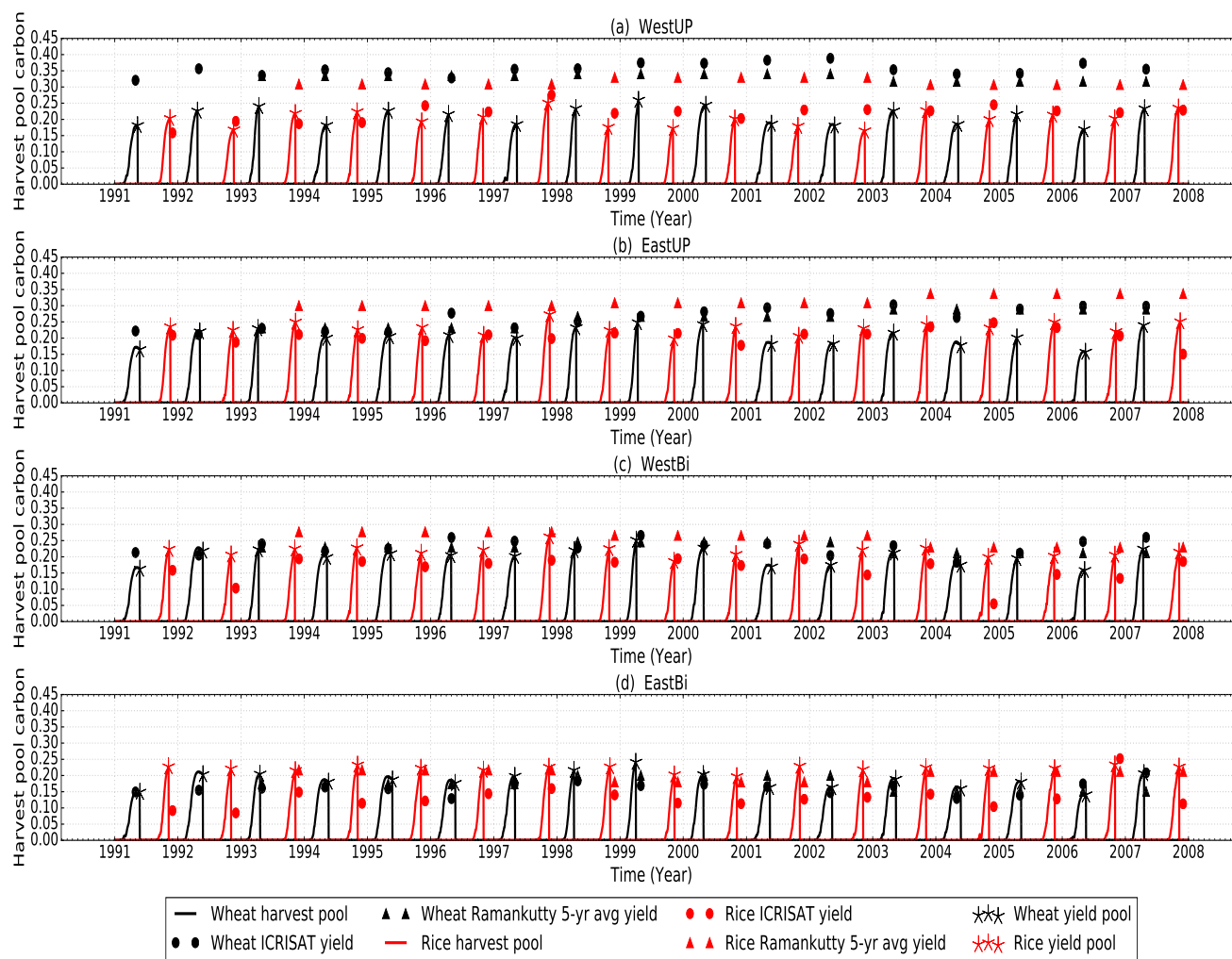


Figure 7. Timeseries of crop harvest pool (solid lines) with the JULES yield at the time it is output by the model (asterisks) for rice (red) and wheat (black) at each of the India sites shown in Fig. 2. Also shown are two sets of observations; annual yields from ICRISAT (2015) shown by the filled circles and 5 year averages from Ray et al. (2012a) shown by the filled triangles (following the same colours with rice shown in red and wheat in black)



India point runs: Leaf area index (LAI)

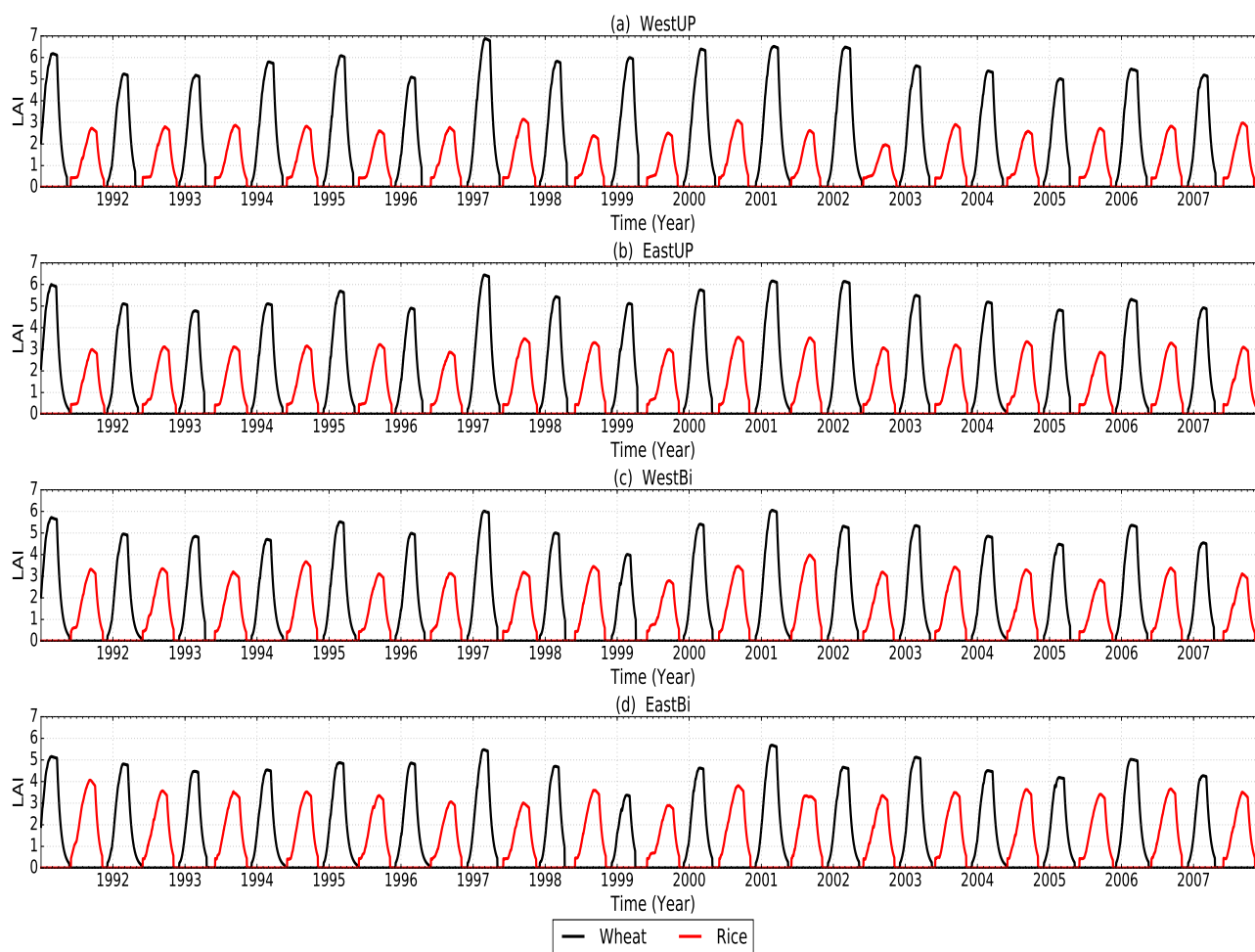


Figure 8. Timeseries of the leaf area index rice (red) and wheat (black) at each of the India sites shown in Fig. 2.



Sequential cropping: Timeseries of each carbon pool (kg m^{-2}) for both rice and wheat

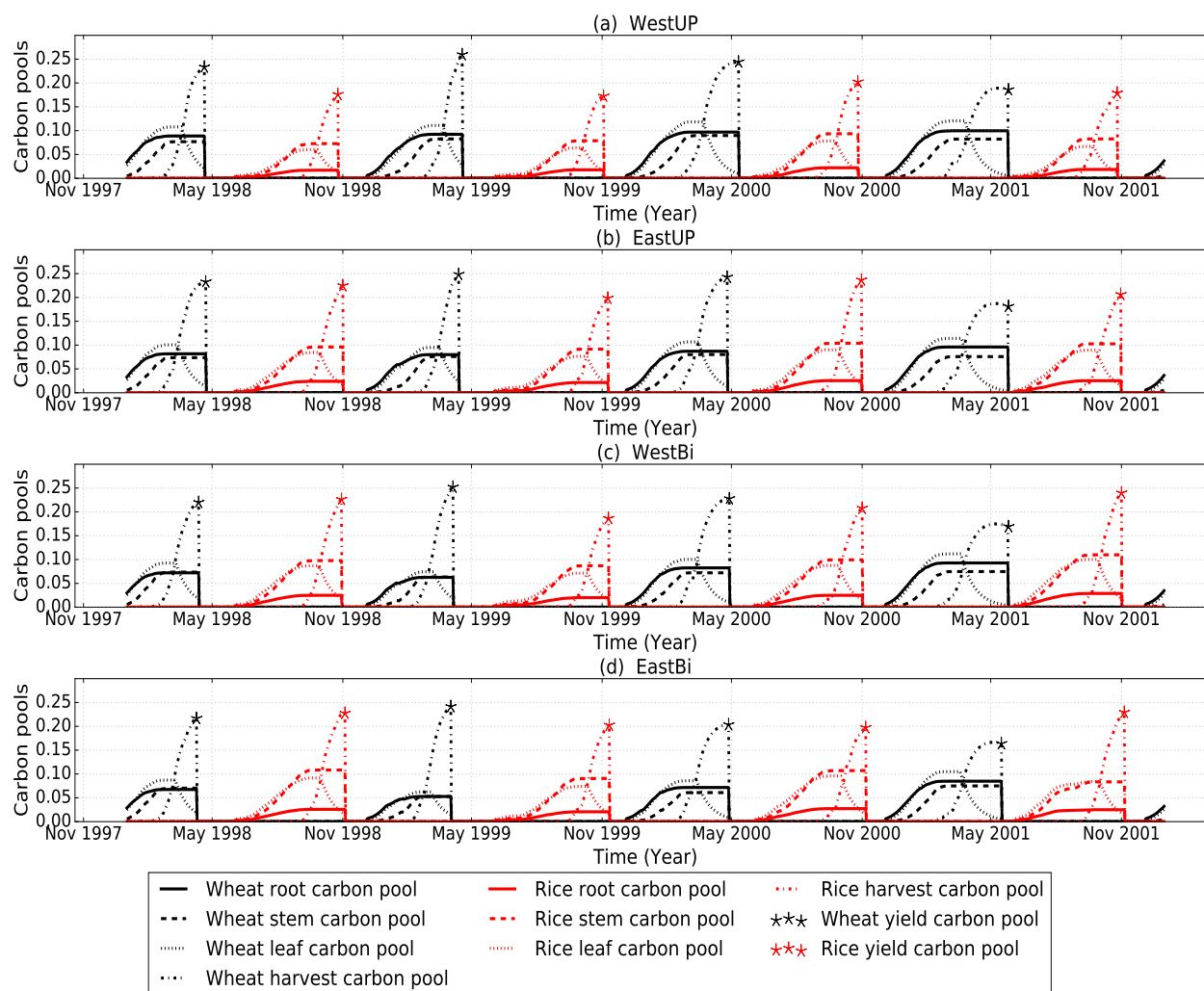


Figure 9. Timeseries of each crop carbon pool: leaf (solid lines), root (dashed), stem (dotted) and harvest (dash-dot) with the JULES yield at the time it is output by the model (asterisks) for rice (red) and wheat (black) at each of the India sites shown in Fig. 2 for a subset of years of the simulation between 1998 and 2001.

The fluxes of heat (LE and H), NPP and GPP are shown for each of the four India locations (see Fig. 2) in Fig. 10, plots (a) to (d), with the moisture fluxes shown in Fig. 11, plot(c). They show the influence of the sequential crop rotation of wheat and rice on the fluxes at each location by the presence of a first peak for wheat and a secondary smaller peak during the rice season. This is most obvious in the plots of NPP and GPP (see Fig. 10, plot (c) and (d) respectively). In general the timeseries of the fluxes shown in Fig. 10 and Fig. 11, plot(c) are quite similar between locations. The timeseries (see Fig. 10) and the



annual cycles (not shown) indicate that on average, all the locations have minima and maxima that occur at the same time. The drier hotter location, WestUP usually has a lower LE , moisture flux and higher H than the other three locations. Although there are two short periods in 1998 and 2001 where EastBi has the lowest available soil moisture, these periods correspond with a lower monsoon rainfall at this location (see Fig. 6). The available soil moisture in the top 1.0 m of soil and the soil

5 moisture availability factor (Beta) are shown in Fig. 11, plot a and b respectively). They show that for several years of the simulation WestUP has the lowest available soil moisture and soil moisture availability factor, suggesting this location is likely to be the most water stressed. WestBi on the other hand often has the highest soil moisture availability factor and the most consistent available soil moisture in the top 1.0 m across the year of the four locations. This is consistent with the temperature and precipitation timeseries shown in Fig. 6 where the locations become wetter and cooler from west to east. This means there

10 is more available soil moisture in the top 1.0 m for the eastern locations compared with the western locations.

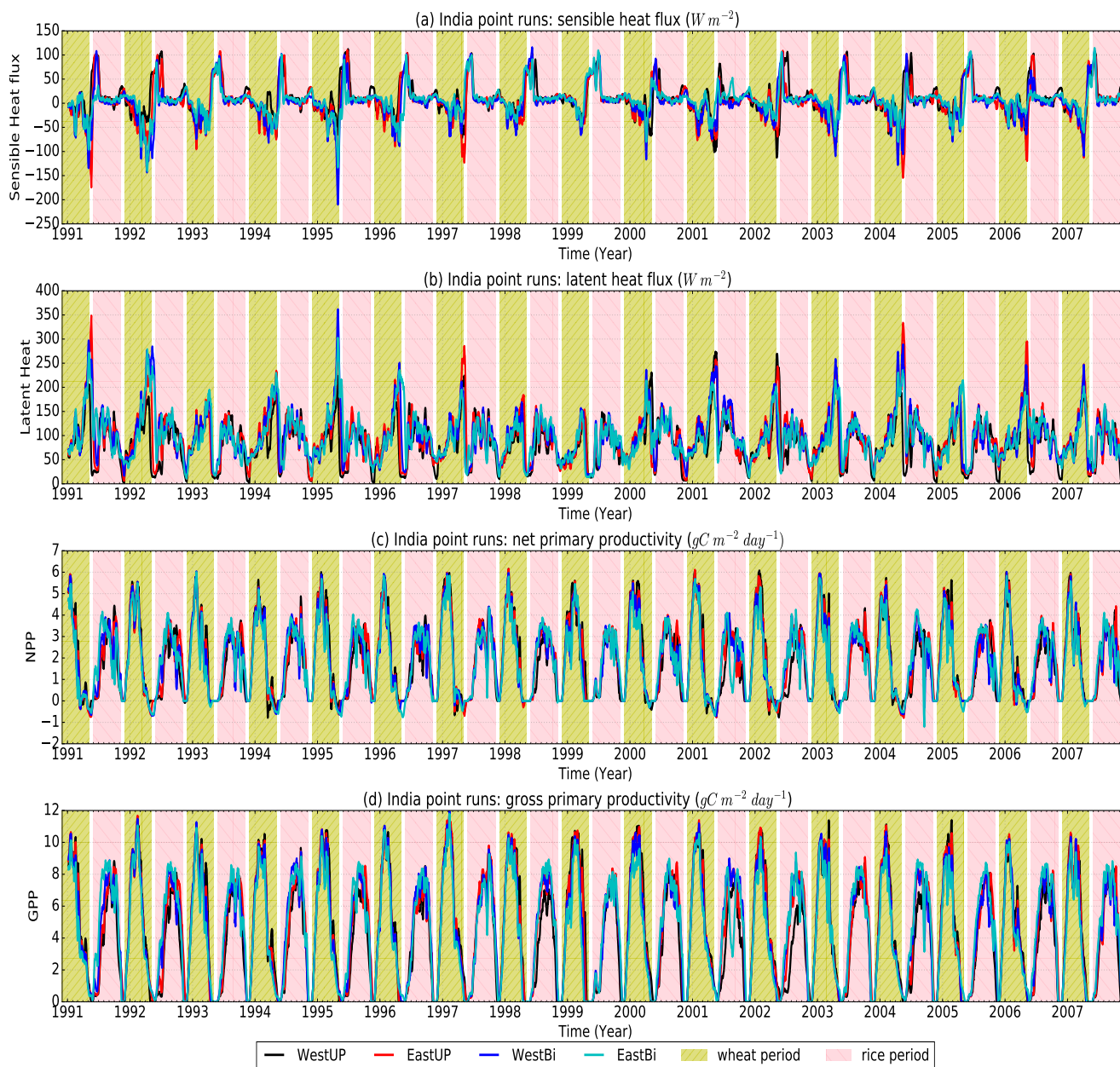


Figure 10. Timeseries of LE (a), H (b), gridbox NPP (c) and gridbox gpp (d) at each of the India sites shown in Fig. 2. Each location is represented by a solid line of a different colour: WestUP - black, EastUP - red, WestBi - blue and EastBi - cyan

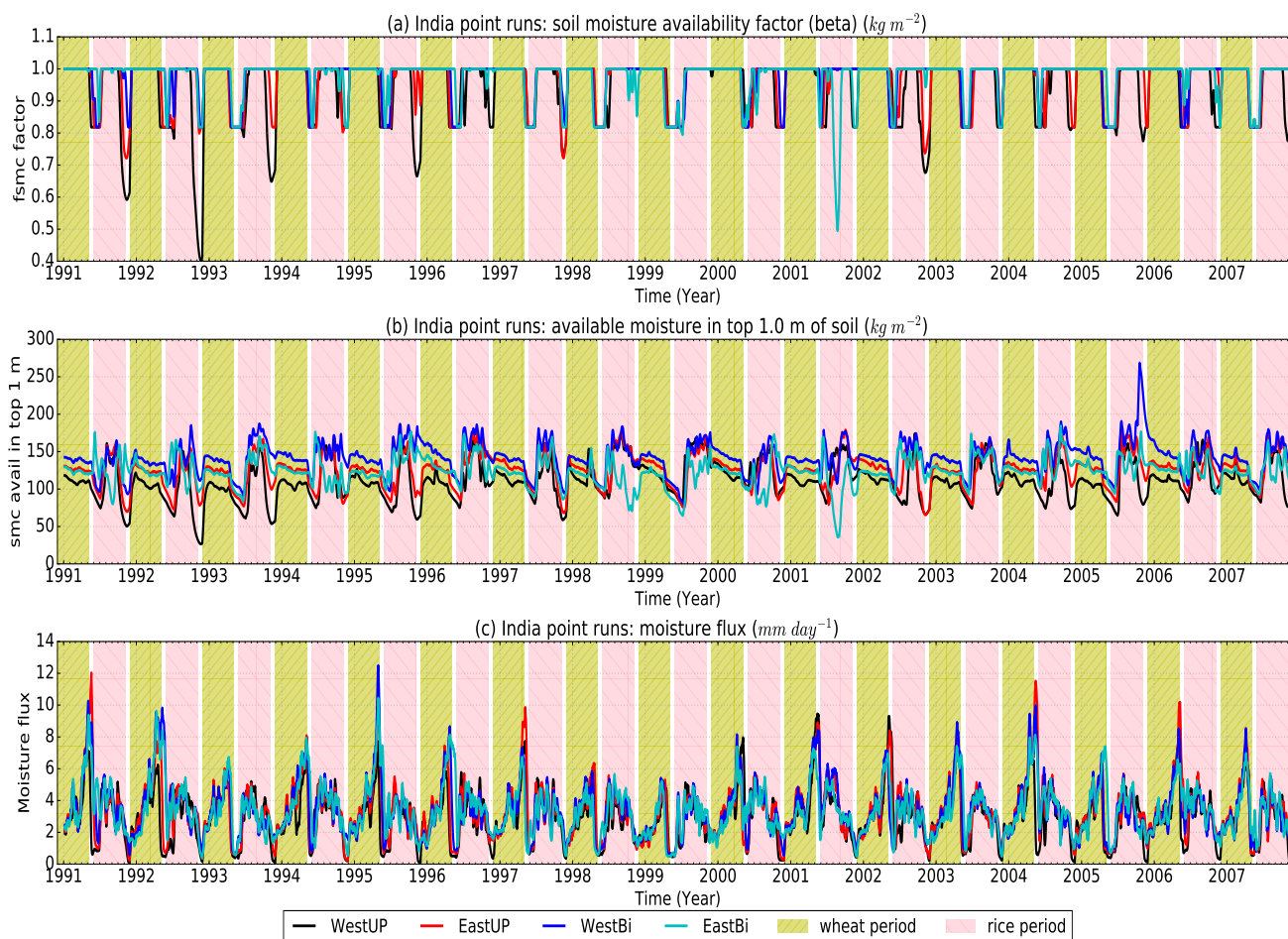


Figure 11. Timeseries of moisture fluxes including the gridbox soil moisture availability factor (beta) (a), the gridbox available moisture in the top 1.0 m of soil (b) and moisture flux across the gridbox (c) at each of the India sites shown in Fig. 2. Each location is represented by a solid line of a different colour: WestUP - black, EastUP - red, WestBi - blue and EastBi - cyan

We have shown that JULES simulates wheat and rice across the four locations, however the varying conditions across these locations affect the model response which subsequently affects the yields produced by JULES. In general the model produces a similar amount of wheat biomass to Avignon but produces yields that are closer to those observed than for Avignon. This could be due to the JULES wheat parameterization being more appropriate for modelling Indian spring wheat than Avignon winter wheat varieties.

7 Discussion and Conclusions

In this paper we describe and demonstrate a new development for JULES enabling more than one crop to be simulated at a given location during a particular growing season, thereby including a sequential cropping capability. There are relatively



few models that are able to simulate sequential cropping but there is a growing need as more regions of the world adopt this cropping system as a viable way of adapting to climate change (Hudson, 2009). We demonstrate the method and evaluate its impact for a site in Avignon; this a site that has grown crops in rotation for several years and therefore has a lengthy and detailed observation record. We use this site to simulate a winter wheat–sorghum rotation in JULES approximated using spring wheat and maize. We apply this same method to four locations that use the sequential cropping system in the northern Indian states of Uttar Pradesh and Bihar, in order to inform its implementation for a regional simulation of South Asia.

We show that JULES is able to simulate two crops in a year both at Avignon and the four locations across Uttar Pradesh and Bihar, producing maxima of LAI, canopy height and biomass at approximately the correct times of the year. The wealth of observations at Avignon also provide the opportunity to gain a better understanding of the effect of sequential cropping on the surface fluxes. For Avignon, the representation of GPP and fluxes (H and LE) correlate well with observations with r -values of above 0.7. However the magnitude of the biomass for wheat is underestimated and LAI is overestimated compared with Avignon observations. The aim of showing the method for Avignon was not to produce perfect representations of the crops but show that the method is able to produce two crops in a single growing period and therefore provide a better representation of the real land surface at Avignon than previously possible using the crop model. In general there are only small differences between using the crop model and using grasses to represent the crops at this site, indicating that both provide a similar representation of the surface fluxes. There are two varieties of sorghum grown at this site and this is apparent from the differences in the JULES simulations presented. Using maize as an approximation for sorghum provides a better representation for the variety grown in 2009 than in either of the 2007 or 2011 seasons. The representation of crops at Avignon could be improved by including crop specific parameterizations of winter wheat and sorghum in the model, although sorghum would probably require two different sets of parameters for a significant improvement because the two varieties grown at the site are so different. The soil moisture observations for Avignon show that there are periods where the soil moisture is very low. In additional simulations with prescribed soil moisture (not shown) soil moisture stress causes a significant drop in GPP which is much earlier than shown in the observations, this is the subject of a wider modelling effort (Williams et al., 2018; Harper et al., in preparation) that aims to improve the response to soil moisture stress in JULES.

The sequential cropping system is used widely in the Tropics especially regions such as Pakistan, India and Bangladesh. In order to apply this method to tropical regions we run JULES at four locations across the Indian states of Uttar Pradesh and Bihar, these are the main producers of rice and wheat in India and use of the rice–spring wheat rotation is prevalent in this region. This region is highly variable, both in terms of temperatures (ranging from 7 to 52 °C) and rainfall (between 0 and 15 mm day⁻¹) with these locations showing a cooling moistening trend from west to east making conditions for growing crops very different across a relatively limited area. JULES produces both a rice and wheat crop at each of the four locations with yields for the locations in the cooler, wetter east of the region closer to observed yields than those in the warmer drier west. We propose two possible reasons for this difference, although in reality both could be contributing factors. One explanation for the differences in observed yields between WestUP and EastBi is the differing management practices between the two states of Uttar Pradesh and Bihar. The western locations are typically more effective at adopting new technology and therefore have higher yields than the eastern locations. This difference from west to east may therefore be reduced by a yield gap parameter.



The difference between the observed and model yields at WestUP may be exacerbated by the lack of irrigation in the forcing data which means that evaporation from surface water due to irrigation is missing in these simulations. Tuinenburg et al. (2014) highlight that this makes a considerable contribution to the overall moisture budget for this region. On this basis we hypothesize that this missing evaporative process has a drying effect on the model atmosphere at the western locations which could be affecting the yields there. In addition to this it is possible that revising the carbon partitioning especially for wheat could have a positive impact on yields. Further investigation is needed to establish the reasons for the model yields at these locations. It would be interesting and useful to follow up this study with further simulations which attempt to account for this missing process, for example, by using alternative driving data that includes irrigation and the subsequent surface evaporation. This would demonstrate if the influence of the evaporation of irrigation water from the surface is a large enough effect to increase the modelled yields for WestUP and maintain the yields for EastBi, where the humidity is usually higher and therefore maybe less influenced by this process.

The work presented here has shown that sequential cropping is an important addition to JULES providing a closer representation of the land surface where crops are grown in rotation. Therefore the code modifications presented as part of this analysis, currently in a branch of JULES at vn5.2, are intended for inclusion in a future official version of JULES. This analysis has provided valuable information for using this sequential cropping method for future regional crop simulations, these regional simulations will be the focus of work that follows this paper. Model intercomparison projects such as AgMIP (Rivington and Koo, 2010; Rosenzweig et al., 2013, 2014) and ISIMIP (Warszawski et al., 2013, 2014) have hugely benefited the crop and land-surface modelling communities by accelerating development and understanding of land surface models. On the basis that this cropping system is likely to be a feature of the future land-surface, not just in the tropics but globally as an adaptation to climate change, we encourage other modelling communities to develop their models to include a sequential cropping capability so that future model intercomparisons can include this and find ways to improve it further.

Code and data availability. The JULES model code used in this paper is available from the Met Office Science Repository Service: <https://code.metoffice.gov.uk/trac> on registering. The version of the model used in this analysis is branched from the JULESvn5.2 trunk code and is therefore an enhanced version of the JULES vn5.2 code: the specific revision including the modifications used in this paper is @13322 which is available from this link: https://code.metoffice.gov.uk/trac/jules/browser/main/branches/dev/camillamathison/vn5.2_croprotate_irrigtiles. The developments contained in this branch will hopefully be implemented into the trunk of JULES in the near future. The regional climate model datasets used will hopefully be available via the Centre for Environmental Data Analysis (CEDA) catalogue. It is hoped that the Avignon rose suite will also be made available in order to aid future model development.



Appendix A: Avignon comparison

Comparison between model and obs at Avignon: gridbox GPP

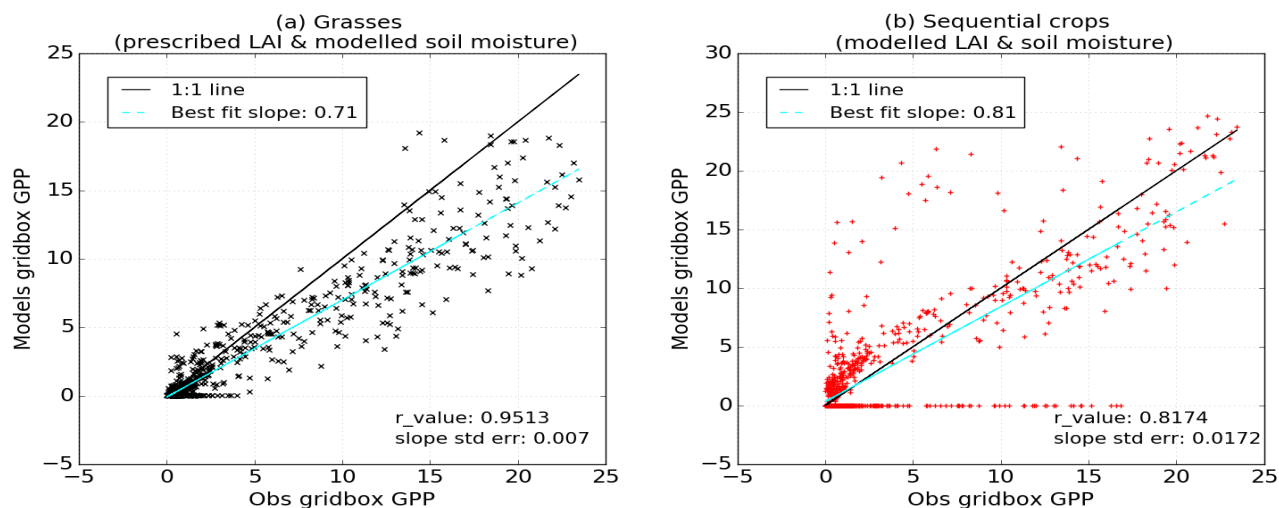


Figure A1. Comparison of Observed GPP at the Avignon site against the modelled GPP between 2005 and 2008 for four simulations: AviJUL-grass with prescribed LAI and modelled soil moisture (a) and AviJUL-sqcrop with both LAI and soil moisture modelled (b)

Comparison between model and obs at Avignon: gridbox sensible heat flux

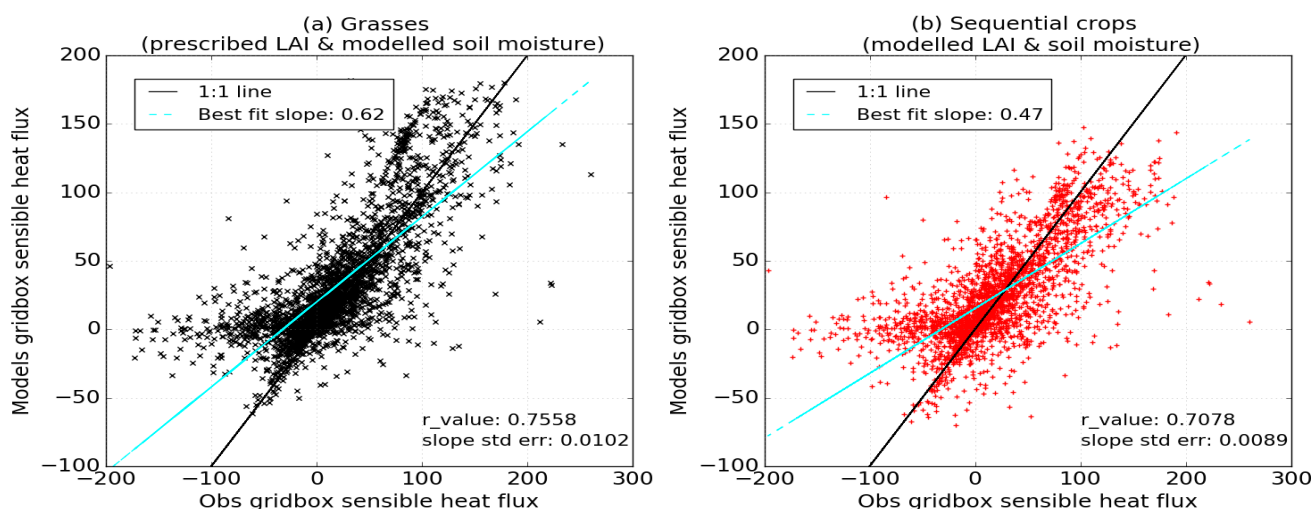


Figure A2. Comparison of observed H at the Avignon site against the modelled H between 2005 and 2013. AviJUL-grass with prescribed LAI and modelled soil moisture (a) and AviJUL-sqcrop with both LAI and soil moisture modelled (b)



Comparison between model and obs at Avignon: gridbox latent heat flux

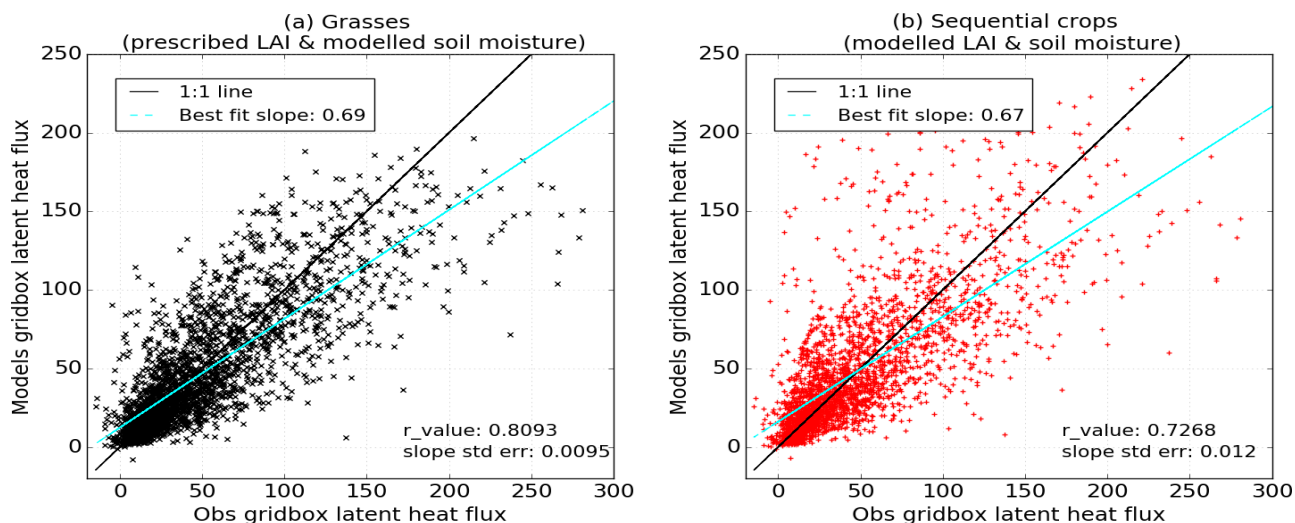


Figure A3. Comparison of observed LE at the Avignon site against the modelled LE between 2005 and 2013. AviJUL-grass with prescribed LAI and modelled soil moisture (a) and AviJUL-sqcrop with both LAI and soil moisture modelled (b).

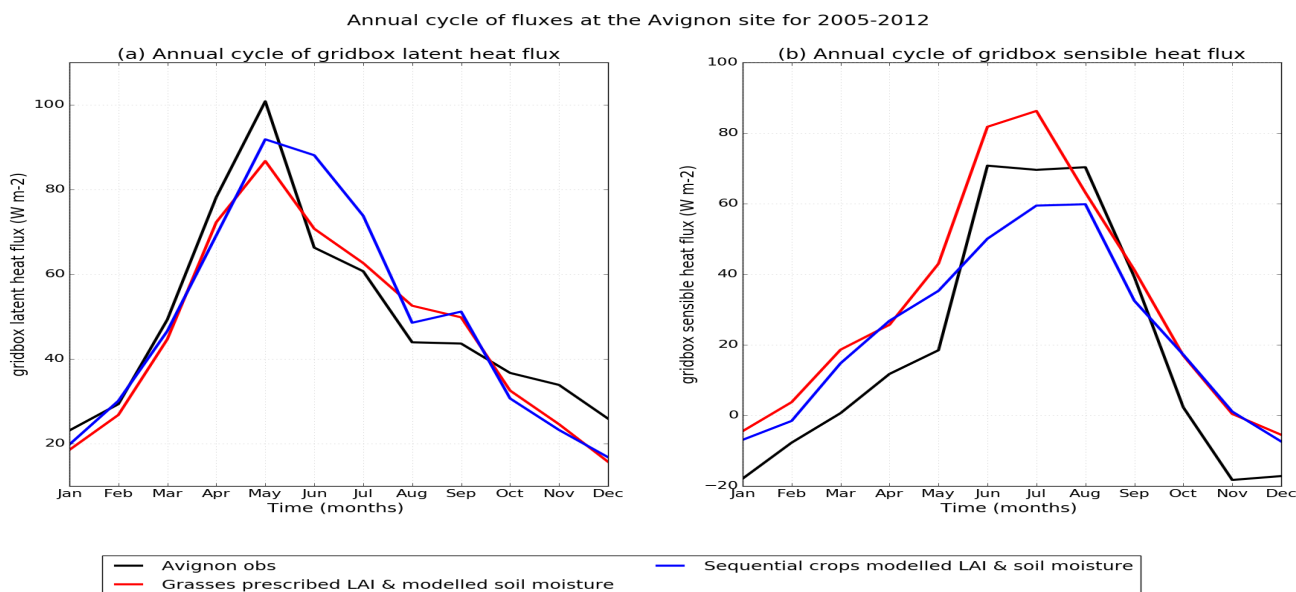


Figure A4. Annual cycle of the H and LE compared with observations (black line) at the Avignon site for between 2005 and 2013. Annual cycles for the simulations are also shown: AviJUL-grass with prescribed LAI and modelled soil moisture (red line). AviJUL-sqcrop with modelled LAI and soil moisture (blue line).

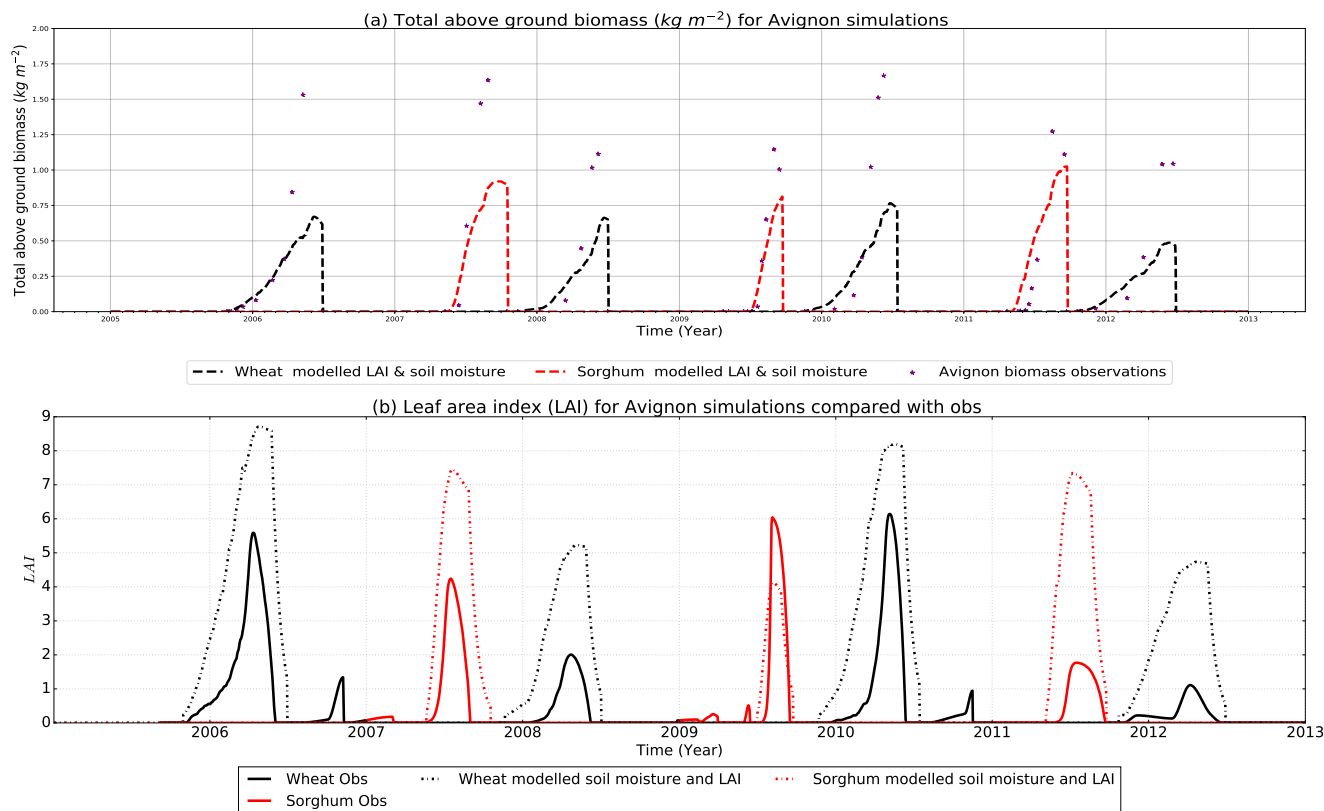


Figure A5. The timeseries of total biomass (a) and leaf area index (LAI) (b) for simulations with a setting of 0 for p_0 for the Avignon site for wheat (black) and sorghum (red) for observations (solid lines) and simulation using the observed sowing and harvest dates: AviJUL-sqcrop (dashed) for the period between 2005 and 2013 using observed sowing and harvest dates. Simulations with prescribed LAI and canopy height are not shown here as these follow the observed LAI and canopy height.



Appendix B: India comparison

Sequential cropping: Total biomass (kg m^{-2}) for both rice and wheat

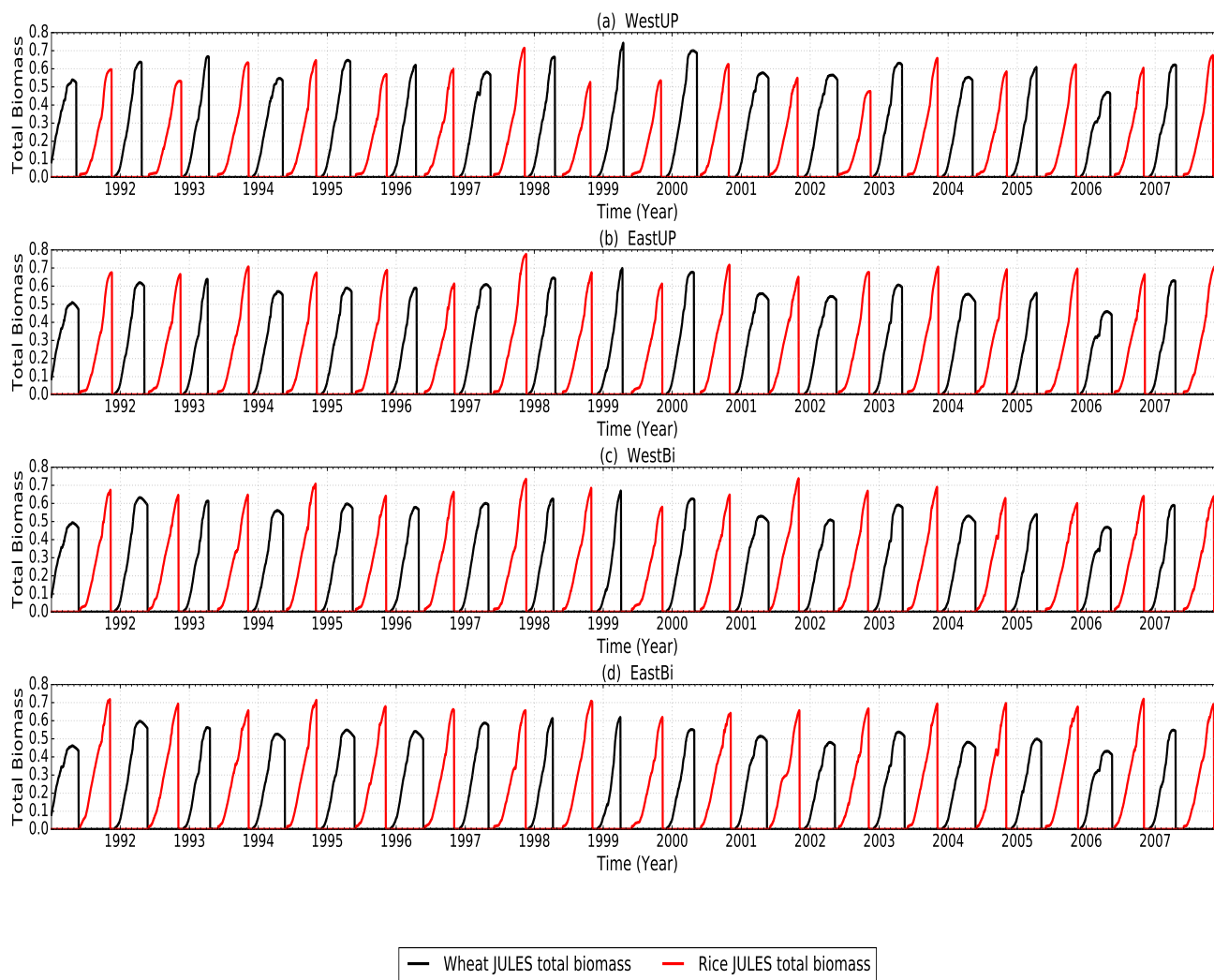


Figure B1. Timeseries of total biomass for rice (red) and wheat (black) at each of the India sites shown in Fig. 2.



India point runs: Development index (DVI)

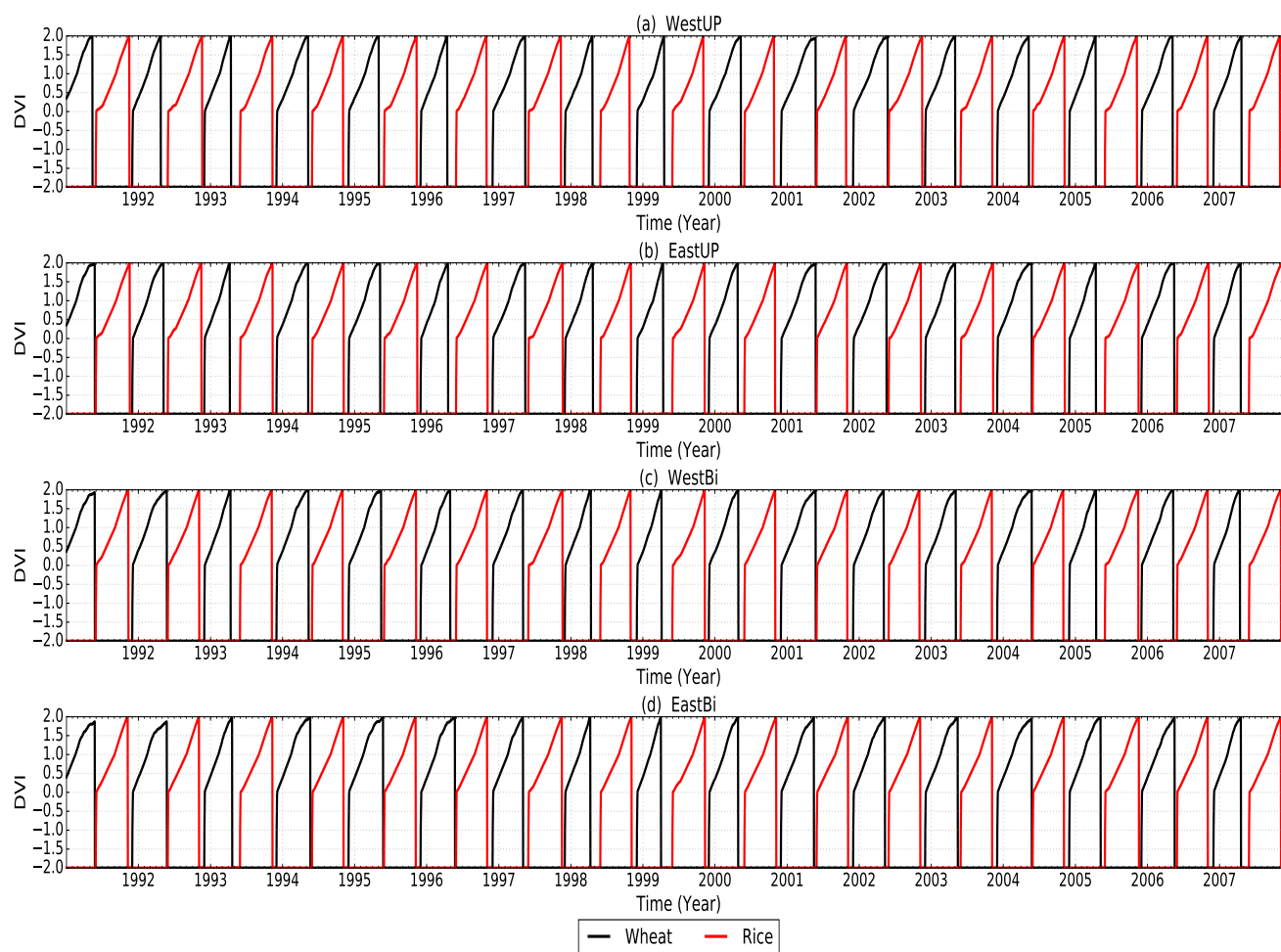


Figure B2. Timeseries of the development index (DVI) for rice (red) and wheat (black) at each of the India sites shown in Fig. 2.



India point runs: Canopy height (m)

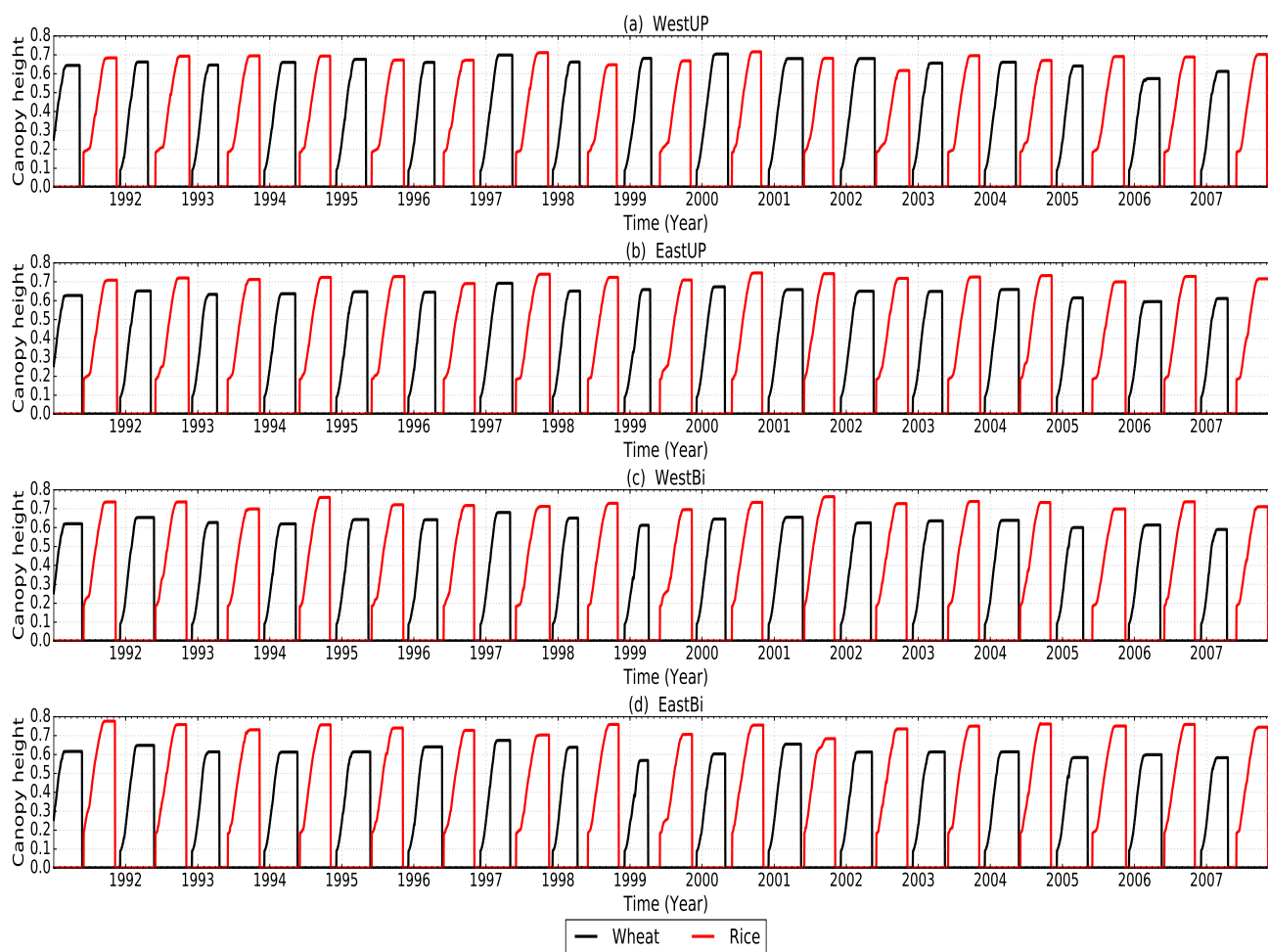


Figure B3. Timeseries of canopy height for rice (red) and wheat (black) at each of the India sites shown in Fig. 2.

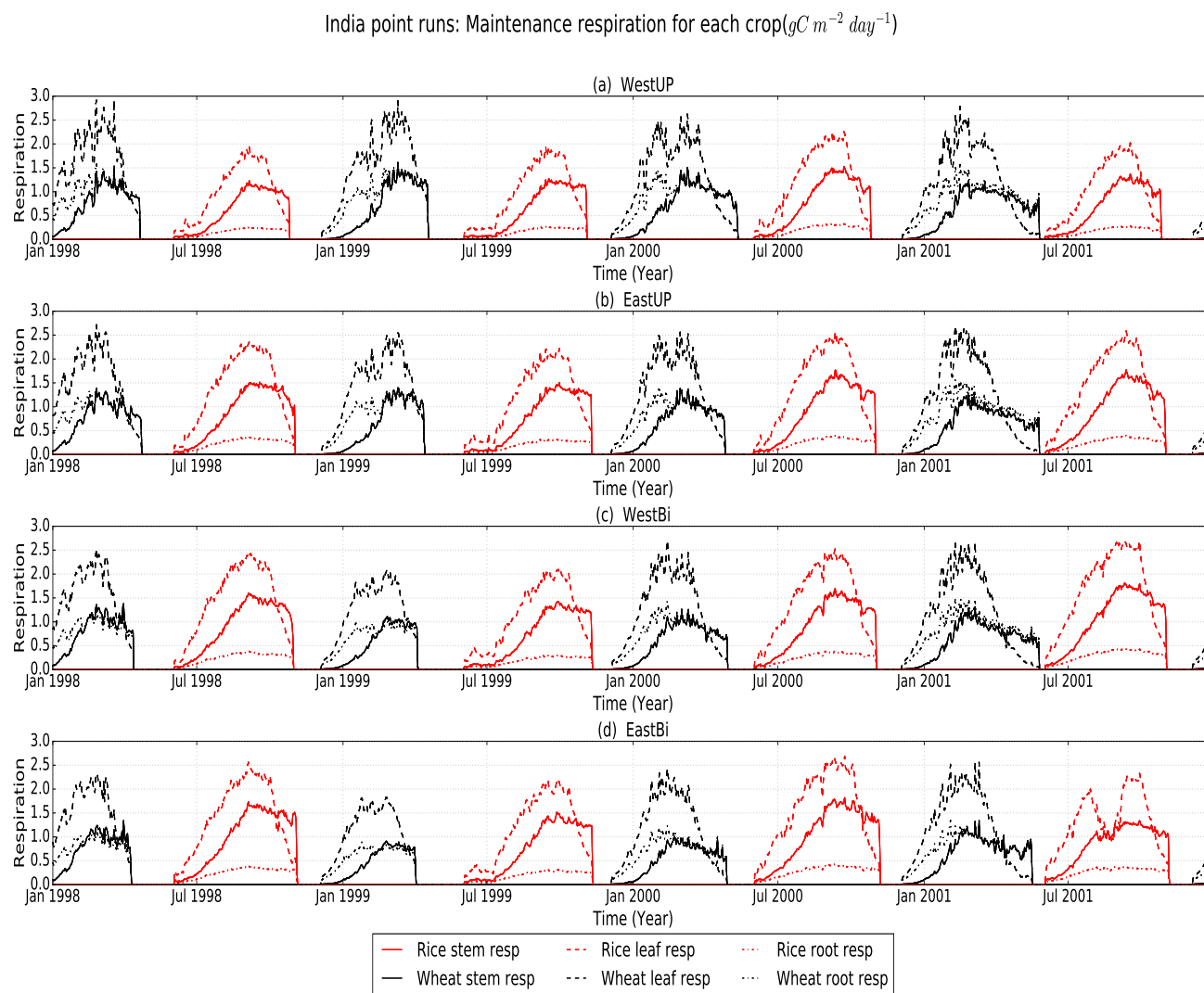


Figure B4. Timeseries of leaf, stem and root leaf respiration for rice (red) and wheat (black) at each of the India sites shown in Fig. 2.

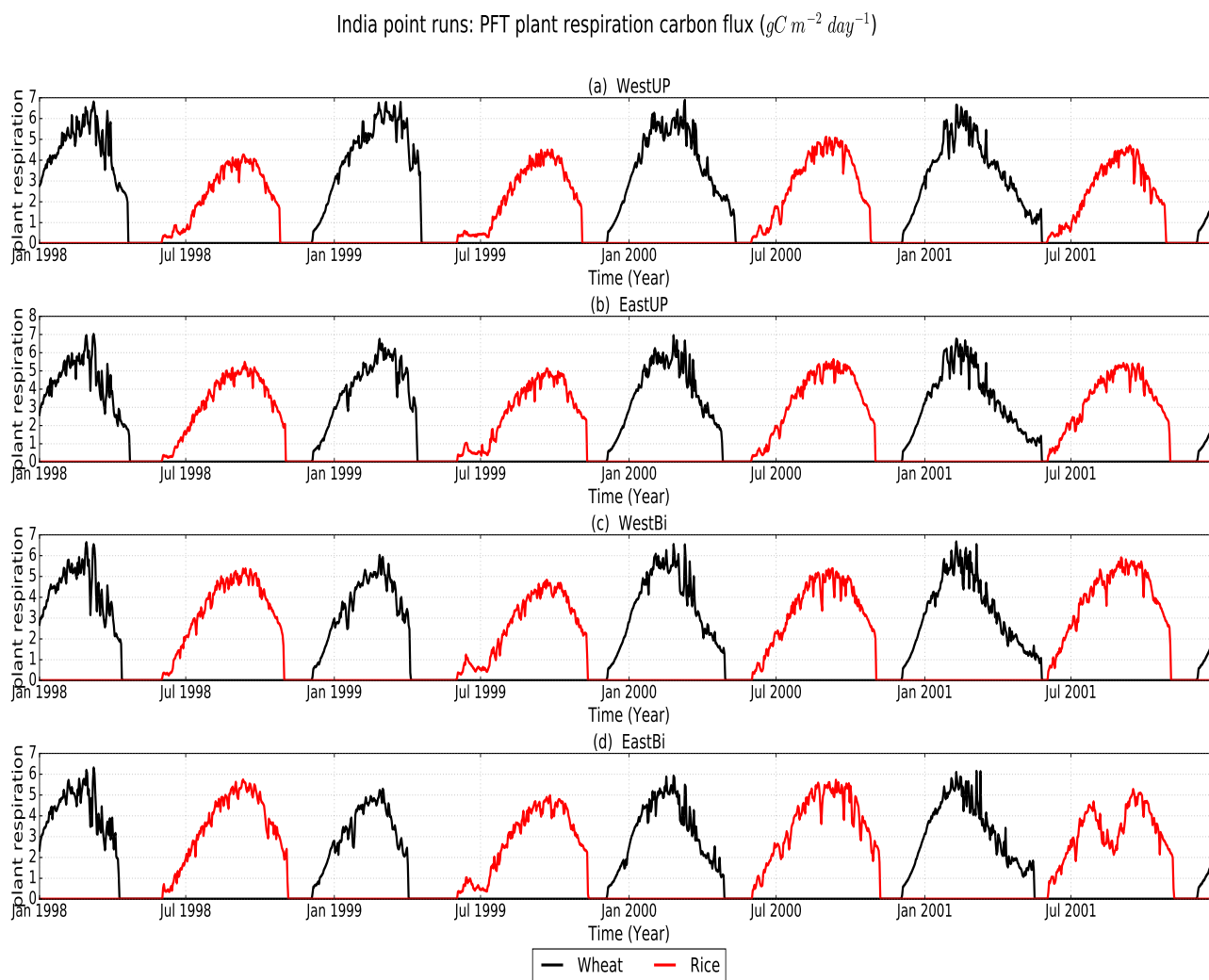


Figure B5. Timeseries of plant respiration for rice (red) and wheat (black) at each of the India sites shown in Fig. 2.

Author contributions. Andrew J Challinor, Pete Falloon and Andy Wiltshire provided general scientific guidance throughout the paper and helped prioritise the initial requirement for including sequential cropping in JULES, toward the aim of modelling integrated impacts for South Asia. Chetan Deva provided gridded observations of crop yield courtesy of ICRISAT. Sébastien Garrigues and Sophie Moulin provided Avignon data. Karina Williams provided code for generating the crop ancillary files and an initial suite for Avignon without crops.



Competing interests. The authors declare that they have no conflict of interest.

Acknowledgements. The research leading to these results has received funding from the European Union Seventh Framework Programme FP7/2007–2013 under grant agreement no. 603864. Camilla Mathison, Pete Falloon, Andy Wiltshire and Karina Williams were supported by the Met Office Hadley Centre Climate Programme funded by BEIS and Defra. Thanks also to Kate Halladay for helping me understand
5 the soil moisture and irrigation implications. The authors thank the INRA EMMAH laboratory at Avignon (France) in charge of the “flux and remote sensing site” for the supply of the data.



References

- Allen, R. G., Pereira, L. S., Raes, D., and Smith, M.: Crop evapotranspiration - Guidelines for computing crop water requirements - FAO Irrigation and drainage paper 56, Food and Agriculture Organization of the United Nations, www.fao.org/3/X0490E/x0490e00.htm, 1998.
- Best, M. J., Pryor, M., Clark, D. B., Rooney, G. G., Essery, R. L. H., Ménard, C. B., Edwards, J. M., Hendry, M. A., Porson, A., Ged-
5 ney, N., Mercado, L. M., Sitch, S., Blyth, E., Boucher, O., Cox, P. M., Grimmond, C. S. B., and Harding, R. J.: The Joint UK Land Environment Simulator (JULES), model description, Part 1: Energy and water fluxes, *Geoscientific Model Development*, 4, 677–699, <https://doi.org/10.5194/gmd-4-677-2011>, <http://www.geosci-model-dev.net/4/677/2011/>, 2011.
- Betts, R. A.: Integrated approaches to climate-crop modelling: needs and challenges, *Philosophical transactions of the Royal Society of London. Series B, Biological sciences*, 360, 2049–65, <https://doi.org/10.1098/rstb.2005.1739>, 2005.
- 10 Bhattacharyya, T., Pal, D., Easter, M., Batjes, N., Milne, E., Gajbhiye, K., Chandran, P., Ray, S., Mandal, C., Paustian, K., Williams, S., Killian, K., Coleman, K., Falloon, P., and Powlson, D.: Modelled soil organic carbon stocks and changes in the Indo-Gangetic Plains, India from 1980 to 2030, *Agriculture, Ecosystems & Environment*, 122, 84 – 94, <https://doi.org/https://doi.org/10.1016/j.agee.2007.01.010>, <http://www.sciencedirect.com/science/article/pii/S0167880907000394>, soil carbon stocks at regional scales, 2007.
- Biemans, H., Speelman, L., Ludwig, F., Moors, E., Wiltshire, A., Kumar, P., Gerten, D., and Kabat, P.: Future water resources for food
15 production in five South Asian river basins and potential for adaptation - A modeling study, *Science of The Total Environment*, 468–469, Supplement, S117–S131, <https://doi.org/http://dx.doi.org/10.1016/j.scitotenv.2013.05.092>, <http://dx.doi.org/10.1016/j.scitotenv.2013.05.092>, 2013.
- Biemans, H., Siderius, C., Mishra, A., and Ahmad, B.: Crop-specific seasonal estimates of irrigation-water demand in South Asia, *Hydrology and Earth System Sciences*, 20, 1971–1982, <https://doi.org/10.5194/hess-20-1971-2016>, 2016.
- 20 Bodh, S. P. C., Rai, S. J. P., Sharma, S. A., Gajria, S. P., Yadav, S. M., Virmani, S. S., and Pandey, S. R.: *Agricultural Statistics at a Glance 2015*, Ministry of Agriculture & Farmers welfare, Directorate of Economics and Statistics, <http://eands.dacnet.nic.in>, 2015.
- Bondeau, A., Smith, P. C., Zaehle, S., Schaphoff, S., Lucht, W., Cramer, W., Gerten, D., Lotze-Campen, H., Müller, C., Reichstein, M., and Smith, B.: Modelling the role of agriculture for the 20th century global terrestrial carbon balance, *Global Change Biology*, 13, 679–706, <https://doi.org/10.1111/j.1365-2486.2006.01305.x>, <https://onlinelibrary.wiley.com/doi/abs/10.1111/j.1365-2486.2006.01305.x>, 2007.
- 25 Caldwell, R. M. and Hansen, J. W.: Simulation of multiple cropping systems with CropSys, pp. 397–412, Springer Netherlands, Dordrecht, https://doi.org/10.1007/978-94-011-2842-1_24, https://doi.org/10.1007/978-94-011-2842-1_24, 1993.
- Calvet, J.-C., Noilhan, J., Roujean, J.-L., Bessemoulin, P., Cabelguenne, M., Olioso, A., and Wigneron, J.-P.: An interactive vegetation SVAT model tested against data from six contrasting sites, *Agricultural and Forest Meteorology*, 92, 73–95, [https://doi.org/10.1016/S0168-1923\(98\)00091-4](https://doi.org/10.1016/S0168-1923(98)00091-4), 1998.
- 30 Challinor, A., Wheeler, T., Craufurd, P., Slingo, J., and Grimes, D.: Design and optimisation of a large-area process-based model for annual crops, *Agricultural and Forest Meteorology*, 124, 99 – 120, <https://doi.org/https://doi.org/10.1016/j.agrformet.2004.01.002>, <http://www.sciencedirect.com/science/article/pii/S0168192304000085>, 2004.
- Clark, D. B., Mercado, L. M., Sitch, S., Jones, C. D., Gedney, N., Best, M. J., Pryor, M., Rooney, G. G., Essery, R. L. H., Blyth, E., Boucher, O., Harding, R. J., Huntingford, C., and Cox, P. M.: The Joint UK Land Environment Simulator (JULES), model description,
35 Part 2: Carbon fluxes and vegetation dynamics, *Geoscientific Model Development*, 4, 701–722, <https://doi.org/10.5194/gmd-4-701-2011>, <http://www.geosci-model-dev.net/4/701/2011/>, 2011.



- Cong, W.-F., Hoffland, E., Li, L., Six, J., Sun, J.-H., Bao, X.-G., Zhang, F.-S., and Werf, W. V. D.: Intercropping enhances soil carbon and nitrogen, *Global Change Biology*, 21, 1715–1726, <https://doi.org/10.1111/gcb.12738>, <https://onlinelibrary.wiley.com/doi/abs/10.1111/gcb.12738>, 2015.
- Dee, D. P., Uppala, S. M., Simmons, A. J., Berrisford, P., Poli, P., Kobayashi, S., Andrae, U., Balmaseda, M. A., P., G. B., Bauer, Bechtold, P.,
5 Beljaars, A. C. M., van de Berg, L., Bidlot, J., Bormann, N., Delsol, C., Dragani, R., Fuentes, M., Geer, A. J., Haimberger, L., Healy, S. B., Hersbach, H., Hólm, E. V., Isaksen, I., Kållberg, P., Köhler, M., Matricardi, M., McNally, A. P., Monge-Sanz, B. M., Morcrette, J.-J., Park, B.-K., Peubey, C., de Rosnay, P., Tavolato, C., Thépaut, J.-N., and Vitart, F.: The ERA-Interim reanalysis: configuration and performance of the data assimilation system, *Quarterly Journal of the Royal Meteorological Society*, 137, 553–597, <https://doi.org/10.1002/qj.828>, <http://dx.doi.org/10.1002/qj.828>, 2011.
- 10 Dury, J., Schaller, N., Garcia, F., Reynaud, A., and Bergez, J. E.: Models to support cropping plan and crop rotation decisions. A review, *Agronomy for Sustainable Development*, 32, 567–580, <https://doi.org/10.1007/s13593-011-0037-x>, <https://doi.org/10.1007/s13593-011-0037-x>, 2012.
- Erenstein, O. and Laxmi, V.: Zero tillage impacts in India's rice-wheat systems: A review, *Soil and Tillage Research*, 100, 1 – 14, <https://doi.org/https://doi.org/10.1016/j.still.2008.05.001>, <http://www.sciencedirect.com/science/article/pii/S0167198708000822>, 2008.
- 15 Erenstein, O., Farooq, U., Malik, R., and Sharif, M.: On-farm impacts of zero tillage wheat in South Asia's rice-wheat systems, *Field Crops Research*, 105, 240–252, <https://doi.org/https://doi.org/10.1016/j.fcr.2007.10.010>, <http://www.sciencedirect.com/science/article/pii/S0378429007002067>, 2008.
- Essery, R. L. H., Best, M. J., and Cox, P. M.: MOSES 2.2 technical documentation, Hadley Centre Technical Note, 30, <http://www.metoffice.gov.uk/archive/hadley-centre-technical-note-30>, 2001.
- 20 Fischer, R.: Definitions and determination of crop yield, yield gaps, and of rates of change, *Field Crops Research*, 182, 9–18, <https://doi.org/10.1016/j.fcr.2014.12.006>, 2015.
- Frieler, K., Levermann, A., Elliott, J., Heinke, J., Arneth, A., Bierkens, M. F. P., Ciais, P., Clark, D. B., Deryng, D., Döll, P., Falloon, P., Fekete, B., Folberth, C., Friend, A. D., Gellhorn, C., Gosling, S. N., Haddeland, I., Khabarov, N., Lomas, M., Masaki, Y., Nishina, K., Neumann, K., Oki, T., Pavlick, R., C.Ruane, A., Schmid, E., Schmitz, C., Stacke, T., Stehfest, E., Tang, Q., Wisser, D., Huber, V., Piontek, F., Warsza-
25 wski, L., Schewe, J., Lotze-Campen, H., and Schellnhuber, H. J.: A framework for the cross-sectoral integration of multi-model impact projections: land use decisions under climate impacts uncertainties, *Earth System Dynamics*, 6, 447–460, <https://doi.org/10.5194/esd-6-447-2015>, <https://www.earth-syst-dynam.net/6/447/2015/>, 2015.
- Garrigues, S., Oliso, A., Calvet, J., Martin, E., Lafont, S., Moulin, S., Chanzy, A., Marloie, O., Buis, S., Desfonds, V., Bertrand, N., and Renard, D.: Evaluation of land surface model simulations of evapotranspiration over a 12-year crop succession: impact of soil hydraulic
30 and vegetation properties, *Hydrology and Earth System Sciences*, 19, 3109–3131, <https://doi.org/10.5194/hess-19-3109-2015>, <https://www.hydrol-earth-syst-sci.net/19/3109/2015/>, 2015.
- Garrigues, S., Boone, A., Decharme, B., Oliso, A., Albergel, C., Calvet, J.-C., Moulin, S., Buis, S., and Martin, E.: Impacts of the Soil Water Transfer Parameterization on the Simulation of Evapotranspiration over a 14-Year Mediterranean Crop Succession, *Journal of Hydrometeorology*, 19, 3–25, <https://doi.org/10.1175/JHM-D-17-0058.1>, <https://doi.org/10.1175/JHM-D-17-0058.1>, 2018.
- 35 Goswami, B. and Xavier, P. K.: Dynamics of "internal" interannual variability of the Indian summer monsoon in a GCM, *Journal of Geophysical Research: Atmospheres*, 110, n/a–n/a, <https://doi.org/10.1029/2005JD006042>, <http://dx.doi.org/10.1029/2005JD006042>, 2005.
- Griffiths, F. E. W., Lyndon, R., and Bennett, M.: The Effects of Vernalization on the Growth of the Wheat Shoot Apex, *Annals of Botany*, 56, 501–511, <https://doi.org/10.1093/oxfordjournals.aob.a087035>, 1985.



- Harding, R., Blyth, E., Tuinenburg, O., and Wiltshire, A.: Land atmosphere feedbacks and their role in the water resources of the Ganges basin, *Science of The Total Environment*, 468-469, Supplement, S85 – S92, <https://doi.org/http://dx.doi.org/10.1016/j.scitotenv.2013.03.016>, <http://www.sciencedirect.com/science/article/pii/S0048969713003070>, changing water resources availability in Northern India with respect to Himalayan glacier retreat and changing monsoon patterns: consequences and adaptation, 2013.
- 5 Harper, A. B., Williams, K., Team, J., and Team, F.: Toward an improved representation of soil moisture stress: disentangling causes and effects, to be decided, 00, 0–34, in preparation.
- Hatfield, J. L. and Prueger, J. H.: Temperature extremes: Effect on plant growth and development, *Weather and Climate Extremes*, 10, 4 – 10, <https://doi.org/https://doi.org/10.1016/j.wace.2015.08.001>, <http://www.sciencedirect.com/science/article/pii/S2212094715300116>, uSDA
- 10 Research and Programs on Extreme Events, 2015.
- Hu, S., Mo, X., and Lin, Z.: Optimizing the photosynthetic parameter V_{cmax} by assimilating MODIS-fPAR and MODIS-NDVI with a process-based ecosystem model, *Agricultural and Forest Meteorology*, 198-199, 320 – 334, <https://doi.org/https://doi.org/10.1016/j.agrformet.2014.09.002>, <http://www.sciencedirect.com/science/article/pii/S0168192314002123>, 2014.
- 15 Hudson, R.: Management of Agricultural, Forestry, Fisheries and Rural Enterprise - Volume I, EOLSS Publications, 2009, <https://books.google.co.uk/books?id=-eGvCwAAQBAJ>, 2009.
- ICRISAT: District Level Database Documentation, Tech. rep., International Crops Research Institute for the Semi-Arid Tropics, Hyderabad, 2015.
- Iizumi, T. and Ramankutty, N.: How do weather and climate influence cropping area and intensity?, *Global Food Security*, 4, 46 – 50, <https://doi.org/https://doi.org/10.1016/j.gfs.2014.11.003>, <http://www.sciencedirect.com/science/article/pii/S2211912414000583>, 2015.
- 20 Jones, R. G., Noguier, M., Hassell, D. C., Hudson, D., Wilson, S. S., Jenkins, G. J., and Mitchell, J. F.: Generating high resolution climate change scenarios using PRECIS, Met Office Hadley Centre, Exeter, UK, pp. 0–40, http://precis.metoffice.com/docs/PRECIS_Handbook.pdf, 2004.
- Kumar, P., Wiltshire, A., Mathison, C., Asharaf, S., Ahrens, B., Lucas-Picher, P., Christensen, J. H., Gobiet, A., Saeed, F., Hagemann, S., and Jacob, D.: Downscaled climate change projections with uncertainty assessment over India using a high resolution multi-model approach, *Science of The Total Environment*, 468-469, Supplement, S18 – S30, <https://doi.org/http://dx.doi.org/10.1016/j.scitotenv.2013.01.051>, <http://www.sciencedirect.com/science/article/pii/S004896971300106X>, changing water resources availability in Northern India with respect to Himalayan glacier retreat and changing monsoon patterns: consequences and adaptation, 2013.
- 25 Kumar, R., Singh, R., and Sharma, K.: Water resources of India, *Current Science*, 89, 794–811, 2005.
- 30 Laik, R., Sharma, S., Idris, M., Singh, A., Singh, S., Bhatt, B., Saharawat, Y., Humphreys, E., and Ladha, J.: Integration of conservation agriculture with best management practices for improving system performance of the rice–wheat rotation in the Eastern Indo-Gangetic Plains of India, *Agriculture, Ecosystems & Environment*, 195, 68–82, <https://doi.org/https://doi.org/10.1016/j.agee.2014.06.001>, <http://www.sciencedirect.com/science/article/pii/S0167880914003211>, 2014.
- Liu, L., Xu, X., Zhuang, D., Chen, X., and Li, S.: Changes in the Potential Multiple Cropping System in Response to Climate Change in China from 1960–2010, *PLoS ONE*, 8, <https://doi.org/https://doi.org/10.1371/JOURNAL.PONE.0080990>, <http://journals.plos.org/plosone/article/file?id=10.1371/journal.pone.0080990&type=printable>, 2013.
- 35 Mahajan, A. and Gupta, R. D., eds.: The Rice–Wheat Cropping System, pp. 109–117, Springer Netherlands, Dordrecht, https://doi.org/10.1007/978-1-4020-9875-8_7, https://doi.org/10.1007/978-1-4020-9875-8_7, 2009.



- Makino, A.: Rubisco and nitrogen relationships in rice: Leaf photosynthesis and plant growth, *Soil Science and Plant Nutrition*, 49, 319–327, <https://doi.org/10.1080/00380768.2003.10410016>, <https://doi.org/10.1080/00380768.2003.10410016>, 2003.
- Mathison, C., Wiltshire, A., Dimri, A., Falloon, P., Jacob, D., Kumar, P., Moors, E., Ridley, J., Siderius, C., Stoffel, M., and Yasunari, T.: Regional projections of North Indian climate for adaptation studies, *Science of The Total Environment*, 468–469, Supplement, S4–S17, <https://doi.org/http://dx.doi.org/10.1016/j.scitotenv.2012.04.066>, <http://www.sciencedirect.com/science/article/pii/S0048969712006377>, 2013.
- Mathison, C., Wiltshire, A. J., Falloon, P., and Challinor, A. J.: South Asia river-flow projections and their implications for water resources, *Hydrology and Earth System Sciences*, 19, 4783–4810, <https://doi.org/10.5194/hess-19-4783-2015>, <http://www.hydrol-earth-syst-sci.net/19/4783/2015/>, 2015.
- 10 Mathison, C., Deva, C., Falloon, P., and Challinor, A. J.: Estimating sowing and harvest dates based on the Asian Summer Monsoon, *Earth System Dynamics*, 9, 563–592, <https://doi.org/10.5194/esd-9-563-2018>, <https://www.earth-syst-dynam.net/9/563/2018/>, 2018.
- Medina, S., Vicente, R., Nieto-Taladriz, M. T., Aparicio, N., Chairi, F., Vergara-Diaz, O., and Araus, J. L.: The plant-transpiration response to vapor pressure deficit (VPD) in Durum Wheat is associated with differential yield performance and specific expression of genes involved in primary metabolism and water transport, *Frontiers in Plant Science*, 9, 1994, <https://doi.org/10.3389/fpls.2018.01994>, 2019.
- 15 Monfreda, C., Ramankutty, N., and Foley, J. A.: Farming the planet: 2. Geographic distribution of crop areas, yields, physiological types, and net primary production in the year 2000, *Global Biogeochemical Cycles*, 22, <https://doi.org/10.1029/2007GB002947>, <https://agupubs.onlinelibrary.wiley.com/doi/abs/10.1029/2007GB002947>, 2008.
- Mueller, B., Hauser, M., Iles, C., Rimi, R. H., Zwiers, F. W., and Wan, H.: Lengthening of the growing season in wheat and maize producing regions, *Weather and Climate Extremes*, 9, 47 – 56, <https://doi.org/https://doi.org/10.1016/j.wace.2015.04.001>, <http://www.sciencedirect.com/science/article/pii/S2212094715000183>, the World Climate Research Program Grand Challenge on Extremes – WCRP-ICTP Summer School on Attribution and Prediction of Extreme Events, 2015.
- 20 Nicklin, K.: Seasonal crop yield forecasting in semi-arid West Africa, PhD thesis, University of Leeds, 1, Chapter 4, 2012.
- Noilhan, J. and Planton, S.: A Simple Parameterization of Land Surface Processes for Meteorological Models, *Monthly Weather Review*, 117, 536–549, [https://doi.org/10.1175/1520-0493\(1989\)117<0536:ASPOLS>2.0.CO;2](https://doi.org/10.1175/1520-0493(1989)117<0536:ASPOLS>2.0.CO;2), 1989.
- 25 Ocheltree, T. W., Nippert, J. B., and Prasad, P. V. V.: Stomatal responses to changes in vapor pressure deficit reflect tissue-specific differences in hydraulic conductance, *Plant, Cell & Environment*, 37, 132–139, <https://doi.org/10.1111/pce.12137>, <https://onlinelibrary.wiley.com/doi/abs/10.1111/pce.12137>, 2014.
- Ogbaga, C.: Regulation of Photosynthesis in Sorghum in response to drought, PhD Thesis, University of Manchester, 1, 1–186, <https://doi.org/10.13140/RG.2.1.4756.5208>, https://www.researchgate.net/profile/Chukwuma_Ogbaga/publication/301364410/inline/jsViewer/5715f74c08ae0f1a39b1b705, 2014.
- 30 Olsovská, K., Kovar, M., Brestic, M., Zivcak, M., Slamka, P., and Shao, H. B.: Genotypically Identifying Wheat Mesophyll Conductance Regulation under Progressive Drought Stress, *Frontiers in Plant Science*, 7, 1111, <https://doi.org/10.3389/fpls.2016.01111>, <https://www.frontiersin.org/article/10.3389/fpls.2016.01111>, 2016.
- Osborne, T., Gornall, J., Hooker, J., Williams, K., Wiltshire, A., Betts, R., and Wheeler, T.: JULES-crop: a parametrisation of crops in the Joint UK Land Environment Simulator, *Geoscientific Model Development*, 8, 1139–1155, <https://doi.org/10.5194/gmd-8-1139-2015>, 2015.
- 35 Penning de Vries, F. W. T., Jansen, D., ten Berge, H., and Bakema, A.: Simulation of Ecophysiological Processes of Growth in Several Annual Crops, *Simulation monographs*, Pudoc, <https://books.google.co.uk/books?id=G-cjxJlr71wC>, 1989.



- Petrie, C. A., Singh, R. N., Bates, J., Dixit, Y., French, C. A. I., Hodell, D. A., Jones, P. J., Lancelotti, C., Lynam, F., Neogi, S., Pandey, A. K., Parikh, D., Pawar, V., Redhouse, D. I., and Singh, D. P.: Adaptation to Variable Environments, Resilience to Climate Change: Investigating Land, Water and Settlement in Indus Northwest India, *Current Anthropology*, 58, 1–30, <https://doi.org/10.1086/690112>, <https://doi.org/10.1086/690112>, 2017.
- 5 Pires, G. F., Abrahão, G. M., Brumatti, L. M., Oliveira, L. J., Costa, M. H., Liddicoat, S., Kato, E., and Ladle, R. J.: Increased climate risk in Brazilian double cropping agriculture systems: Implications for land use in Northern Brazil, *Agricultural and Forest Meteorology*, 228–229, 286 – 298, <https://doi.org/https://doi.org/10.1016/j.agrformet.2016.07.005>, <http://www.sciencedirect.com/science/article/pii/S0168192316303318>, 2016.
- Portmann, F. T., Siebert, S., and Döll, P.: MIRCA2000-Global monthly irrigated and rainfed crop areas around the year
10 2000: A new high-resolution data set for agricultural and hydrological modeling, *Global Biogeochemical Cycles*, 24, n/a–n/a, <https://doi.org/10.1029/2008GB003435>, <http://dx.doi.org/10.1029/2008GB003435>, gB1011, 2010.
- Ramankutty, N., Evan, A. T., Monfreda, C., and Foley, J. A.: Farming the planet: 1. Geographic distribution of global agricultural lands in the year 2000, *Global Biogeochemical Cycles*, 22, n/a–n/a, <https://doi.org/10.1029/2007GB002952>, <http://dx.doi.org/10.1029/2007GB002952>, 2008.
- 15 Ray, D. K., Ramankutty, N., and and, N. D. M.: Recent patterns of crop yield growth and stagnation., *Nature Communications*, 3, 1293–1300, <https://doi.org/10.1038/ncomms2296>, 2012a.
- Ray, D. K., Ramankutty, N., Mueller, N. D., West, P. C., and Foley, J. A.: Harvested Area and Yield for 4 Crops (1995–2005), <http://www.earthstat.org/harvested-area-yield-4-crops-1995-2005/>, 2012b.
- Rivington, M. and Koo, J.: Report on the Meta-Analysis of Crop Modelling for Climate Change and Food Security Survey, Climate Change,
20 Agriculture and Food Security Challenge Program of the CGIAR, <https://cgspace.cgiar.org/rest/bitstreams/9114/retrieve>, 2010.
- Robertson, M., Brooking, I., and Ritchie, J.: Temperature Response of Vernalization in Wheat: Modelling the Effect on the Final Number of Mainstem Leaves, *Annals of Botany*, 78, 371–381, <https://doi.org/10.1006/anbo.1996.0132>, 1996.
- Rosenzweig, C., Jones, J., Hatfield, J., Ruane, A., Boote, K., Thorburn, P., Antle, J., Nelson, G., Porter, C., Janssen, S., Asseng, S., Basso, B., Ewert, F., Wallach, D., Baigorria, G., and Winter, J.: The Agricultural Model Intercompari-
25 son and Improvement Project (AgMIP): Protocols and pilot studies, *Agricultural and Forest Meteorology*, 170, 166 – 182, <https://doi.org/http://dx.doi.org/10.1016/j.agrformet.2012.09.011>, <http://www.sciencedirect.com/science/article/pii/S0168192312002857>, agricultural prediction using climate model ensembles, 2013.
- Rosenzweig, C., Elliott, J., Deryng, D., Ruane, A. C., Müller, C., Arneth, A., Boote, K. J., Folberth, C., Glotter, M., Khabarov, N., Neumann, K., Piontek, F., Pugh, T. A. M., Schmid, E., Stehfest, E., Yang, H., and Jones, J. W.: Assessing agricultural risks of climate change in
30 the 21st century in a global gridded crop model intercomparison, *Proceedings of the National Academy of Sciences*, 111, 3268–3273, <https://doi.org/10.1073/pnas.1222463110>, <http://www.pnas.org/content/111/9/3268.abstract>, 2014.
- Sacks, W. J., Deryng, D., Foley, J. A., and Ramankutty, N.: Crop planting dates: an analysis of global patterns, *Global Ecology and Biogeography*, 19, 607–620, 2010.
- Sharma, B. and Sharma, H.: Status of Rice Production in Assam, India, *Journal of Rice Research*:
35 Open Access, 3, 3–e121, <https://doi.org/10.4172/2375-4338.1000e121>, <https://www.omicsonline.org/open-access/status-of-rice-production-in-assam-india-2375-4338-1000121.pdf>, 2015.
- Simmons, A., Uppala, S., Dee, D., and Kobayashi, S.: ERA-Interim: New ECMWF reanalysis products from 1989 onwards., *ECMWF Newsletter - Winter 2006/07*, 110, 25–35, 2007.



- Sinclair, T., Jr, P. P., Kimball, B., Adamsen, F., LaMorte, R., Wall, G., Hunsaker, D., Adam, N., Brooks, T., Garcia, R., Thompson, T., Leavitt, S., and Matthias, A.: Leaf nitrogen concentration of wheat subjected to elevated [CO₂] and either water or N deficits, *Agriculture, Ecosystems & Environment*, 79, 53 – 60, [https://doi.org/https://doi.org/10.1016/S0167-8809\(99\)00146-2](https://doi.org/https://doi.org/10.1016/S0167-8809(99)00146-2), <http://www.sciencedirect.com/science/article/pii/S0167880999001462>, 2000.
- 5 Streck, N. A.: Stomatal response to water vapor pressure deficit: an unsolved issue, *Current Agricultural Science and Technology*, 9, 2003.
- Tuinenburg, O. A., Hutjes, R. W. A., Stacke, T., Wiltshire, A., and Lucas-Picher, P.: Effects of irrigation in india on the atmospheric water budget., *Journal of Hydrometeorology*, 15, 1028–1050, <https://doi.org/10.1175/JHM-D-13-078.1>, 2014.
- Waha, K., van Bussel, L. G. J., Müller, C., and Bondeau, A.: Climate-driven simulation of global crop sowing dates, *Global Ecology and Biogeography*, 21, 247–259, <https://doi.org/10.1111/j.1466-8238.2011.00678.x>, <http://dx.doi.org/10.1111/j.1466-8238.2011.00678.x>,
10 2012.
- Waha, K., Müller, C., Bondeau, A., Dietrich, J., Kurukulasuriya, P., Heinke, J., and Lotze-Campen, H.: Adaptation to climate change through the choice of cropping system and sowing date in sub-Saharan Africa, *Global Environmental Change*, 23, 130 – 143, <https://doi.org/https://doi.org/10.1016/j.gloenvcha.2012.11.001>, <http://www.sciencedirect.com/science/article/pii/S095937801200132X>, 2013.
- 15 Warszawski, L., Friend, A., Ostberg, S., Frieler, K., Lucht, W., Schaphoff, S., Beerling, D., Cadule, P., Ciais, P., Clark, D. B., Kahana, R., Ito, A., Keribin, R., Kleidon, A., Lomas, M., Nishina, K., Pavlick, R., Rademacher, T. T., Buechner, M., Piontek, F., Schewe, J., Serdeczny, O., and Schellnhuber, H. J.: A multi-model analysis of risk of ecosystem shifts under climate change, *Environmental Research Letters*, 8, 044 018, <http://stacks.iop.org/1748-9326/8/i=4/a=044018>, 2013.
- Warszawski, L., Frieler, K., Huber, V., Piontek, F., Serdeczny, O., and Schewe, J.: The Inter-Sectoral Impact Model In-
20 tercomparison Project (ISI-MIP): Project framework, *Proceedings of the National Academy of Sciences*, 111, 3228–3232, <https://doi.org/10.1073/pnas.1312330110>, <http://www.pnas.org/content/111/9/3228.abstract>, 2014.
- Williams, K., Gornall, J., Harper, A., Wiltshire, A., Hemming, D., Quaife, T., Arkebauer, T., and Scoby, D.: Evaluation of JULES-crop performance against site observations of irrigated maize from Mead, Nebraska, *Geoscientific Model Development*, 10, 1291–1320, <https://doi.org/10.5194/gmd-10-1291-2017>, <https://www.geosci-model-dev.net/10/1291/2017/>, 2017.
- 25 Williams, K. E., Harper, A. B., Huntingford, C., Mercado, L. M., Mathison, C. T., Falloon, P. D., Cox, P. M., and Kim, J.: Revisiting the First ISLSCP Field Experiment to evaluate water stress in JULESv5.0, *Geoscientific Model Development Discussions*, 2018, 1–47, <https://doi.org/10.5194/gmd-2018-210>, <https://www.geosci-model-dev-discuss.net/gmd-2018-210/>, 2018.
- Xue, W.: Evaluation of biophysical factors driving temporal variations in C gain, water use and yield production in Rice, PhD thesis, Department of Plant Ecology, University of Bayreuth, 1, 1–230, https://www.researchgate.net/publication/295562013_Evaluation_of_biophysical_factors_driving_temporal_variations_in_carbon_gain_water_use_and_yield_production_in_rice, 2015.
30
- Zhang, G., Dong, J., Zhou, C., Xu, X., Wang, M., Ouyang, H., and Xiao, X.: Increasing cropping intensity in response to climate warming in Tibetan Plateau, China, *Field Crops Research*, 142, 36 – 46, <https://doi.org/https://doi.org/10.1016/j.fcr.2012.11.021>, <http://www.sciencedirect.com/science/article/pii/S0378429012004091>, 2013.



| Flag | JULES notation | Avignon settings | India settings | Effect of switch |
|------------------------------------|------------------------|------------------|----------------|---|
| Canopy radiation scheme | can_rad_mod | 6 | 6 | Selects the canopy radiation scheme. |
| Irrigation demand | l_irrig_dmd | F | T | Switches on irrigation demand. |
| Irrigation scheme | irr_crop | - | 2 | Irrigation occurs when the development index of the crop is greater than 0. |
| Physiology | l_trait_phys | F | F | Switches on trait based physiology when true. |
| Sowing | l_prescsow | T | T | Selects prescribed sowing. |
| Plant maintenance respiration | l_scale_resp_pm | F | F | Switch to scale respiration by water stress factor. If false this is leaf respiration only but if true includes all plant maintenance respiration. |
| Crop rotation | l_croprotate | T | T | A new switch to use the sequential cropping capability. |
| Irrigation on tiles | frac_irrig_all_tiles | - | F | Switch to allow irrigation on all or specific tiles |
| Irrigation on specific tiles | set_irrfac_on_irrtiles | - | T | A new switch to set irrigation to only occur on a specific tile. |
| Specify irrigated tile(s) | irrigtiles | - | 6 | Setting to set the value(s) of the specific tile(s) to be irrigated. |
| Number of tiles irrigated | nirrtile | - | 1 | Setting to set how many tile(s) to be irrigated. |
| Set a constant irrigation fraction | const_irrfac_irrtiles | - | 1.0 | A new setting to set the value(s) of the irrigation fraction for specific tile(s) to be irrigated in the absence of a file of irrigation fractions. |

Table 1. JULES flags used that are new or different from those in Osborne et al. (2015)



| Parameter | JULES notation | Description | Winter wheat | Sorghum | Spring wheat | Rice |
|---------------|----------------|---|--------------|---------|--------------|---------|
| T_{low} | t_low_io | Lower temperature for photosynthesis ($^{\circ}\text{C}$). | 5 | 18 | 5 | 15 |
| T_{upp} | t_upp_io | Upper temperature for photosynthesis ($^{\circ}\text{C}$). | 30 | 53 | 30 | 40 |
| n_{eff} | neff_io | Scale factor relating V_{cmax} with leaf nitrogen concentration. | 0.8e-3 | 0.75e-3 | 0.8e-3 | 0.95e-3 |
| $n_l(0)$ | nl0_io | Top leaf nitrogen concentration (kg N/kg C). | 0.073 | 0.07 | 0.073 | 0.073 |
| fsmc method | fsmc_mod_io | When equal to 0 we assume an exponential root distribution with depth. When equal to 1, the soil moisture availability factor, fsmc, is calculated using average properties for the root zone. | 1 | 1 | 0 | 0 |
| d_r | rootd_ft_io | If fsmc_mod_io = 0 d_r is the e-folding depth. If fsmc_mod_io = 1 d_r is the total depth of the root zone. | 1.5 | 1.5 | 0.5 | 0.5 |
| $p0$ | fsmc_p0_io | Parameter governing the threshold at which the plant starts to experience water stress due to lack of water in the soil. | 0.5 | 0.5 | 0.5 | 0.5 |
| μ_{rl} | nr_nl_io | Ratio of root nitrogen concentration to leaf nitrogen concentration. | 0.39 | 0.39 | 0.39 | 0.39 |
| μ_{sl} | ns_nl_io | Ratio of stem nitrogen concentration to leaf nitrogen concentration. | 0.43 | 0.43 | 0.43 | 0.43 |
| $Q_{10,leaf}$ | q10_leaf_io | Q_{10} factor in the V_{cmax} calculation. | 1.0 | 1.0 | 1.0 | 1.0 |

Table 2. JULES plant functional type (PFT) parameters and values modified for use in this study. We include only the values that have been changed or are new in JULES since Osborne et al. (2015).



| Parameter | JULES notation | Description | Winter wheat | Sorghum | Spring wheat | Rice |
|--------------|-------------------|--|--------------|---------|--------------|---------|
| T_b | t_bse_io | Base temperature ($^{\circ}\text{K}$). | 273.15 | 284.15 | 273.15 | 278.15 |
| T_m | t_max_io | Max temperature ($^{\circ}\text{K}$). | 303.15 | 317.15 | 308.15 | 315.15 |
| T_o | t_opt_io | Optimum temperature ($^{\circ}\text{K}$). | 293.15 | 305.15 | 293.15 | 303.15 |
| TT_{emr} | tt_emr_io | Thermal time between sowing and emergence ($^{\circ}\text{Cd}$). | 35 | 80 | 35 | 60 |
| TT_{veg} | tt_veg_io | Thermal time between emergence and flowering ($^{\circ}\text{Cd}$). | Table 4 | Table 4 | Table 5 | Table 5 |
| TT_{rep} | tt_rep_io | Thermal time between flowering and maturity ($^{\circ}\text{Cd}$). | Table 4 | Table 4 | Table 5 | Table 5 |
| T_{mort} | t_mort_io | Soil temperature (2^{nd} level) at which to kill crop if $\text{DVI} > 1$ ($^{\circ}\text{K}$). | 273.15 | 281.15 | 273.15 | 281.15 |
| f_{yield} | yield_frac_io | Fraction of the harvest carbon pool converted to yield carbon. | 1.0 | 1.0 | 1.0 | 1.0 |
| DVI_{init} | initial_c_dvi_io | DVI at which the crop carbon is set to C_{init} . | 0.0 | 0.0 | 0.0 | 0.0 |
| DVI_{sen} | sen_dvi_io | DVI at which leaf senescence begins. | 1.5 | 1.5 | 1.5 | 1.5 |
| C_{init} | initial_carbon_io | Carbon in crop at emergence in kgC/m^2 . | 0.01 | 0.01 | 0.01 | 0.01 |

Table 3. JULES crop parameters used in this study. The Sorghum cardinal temperatures are from Nicklin (2012) with the other parameters those used for Maize in Osborne et al. (2015). We include only the values that have been changed or added since Osborne et al. (2015). Table 3 of Osborne et al. (2015) provides the original PFT parameters and Table 4 of Osborne et al. (2015) provides the original crop parameters).



| Year | Crop | Sowing date | Harvest date | Emergence-flowering | Flowering-maturity | Sowing DOY |
|------|--------------|-------------|--------------|---------------------|--------------------|------------|
| 2005 | Winter wheat | 27 Oct 2005 | | 1301.3 | 867.5 | 300 |
| 2006 | | | 27 Jun 2006 | | | |
| 2007 | Sorghum | 10 May 2007 | 16 Oct 2007 | 647.6 | 791.5 | 130 |
| 2007 | Winter wheat | 13 Nov 2007 | | 1401.0 | 934.0 | 317 |
| 2008 | | | 1 Jul 2008 | | | |
| 2009 | Sorghum | 25 Jun 2009 | 22 Sep 2009 | 462.5 | 565.3 | 176 |
| 2009 | Winter wheat | 19 Nov 2009 | | 1308.6 | 872.4 | 323 |
| 2010 | | | 13 Jul 2010 | | | |
| 2011 | Sorghum | 22 Apr 2011 | 22 Sep 2011 | 679.5 | 830.5 | 112 |
| 2011 | Winter wheat | 19 Oct 2011 | | 1559.6 | 1039.7 | 292 |
| 2012 | | | 25 Jun 2012 | | | |

Table 4. Thermal times in degree days used in this study for the Avignon site, these are based on the observed sowing and harvest dates from Garrigues et al. (2015).



| Location | Crop | Sowing DOY | Emergence-flowering | Flowering-maturity |
|----------|--------------|------------|---------------------|--------------------|
| WestUP | Spring wheat | 335 | 1007.6 | 671.1 |
| | Rice | 150 | 1759.4 | 1181.3 |
| EastUP | Spring wheat | 335 | 993.55 | 662.5 |
| | Rice | 150 | 1865.5 | 1243.5 |
| WestBi | Spring wheat | 335 | 991.54 | 661.6 |
| | Rice | 150 | 1907.55 | 1271.7 |
| EastBi | Spring wheat | 335 | 1019.21 | 679.1 |
| | Rice | 150 | 1976.96 | 1300.64 |

Table 5. The sowing day of year (Sowing DOY) and thermal times in degree days used in this study for the locations in Uttar Pradesh and Bihar, India (see 2 for a map of the locations), the values given here are based on the observed sowing and harvest dates from Bodh et al. (2015)



| Variable | Simulation type | RMSE | Bias | r_value |
|-----------|-----------------|------|------|---------|
| GPP | AviJUL-grass | 2.0 | -1.0 | 0.95 |
| | AviJUL-sqcrop | 3.0 | 0.0 | 0.82 |
| <i>H</i> | AviJUL-grass | 37.0 | 13.0 | 0.76 |
| | AviJUL-sqcrop | 38.0 | 6.0 | 0.71 |
| <i>LE</i> | AviJUL-grass | 28.0 | -3.0 | 0.81 |
| | AviJUL-sqcrop | 33.0 | 0.0 | 0.73 |

Table 6. Table of statistics comparing the JULES simulations with and without soil moisture prescribed to observations